SKB TECHNICAL REPORT **91-62**

The kinetics of pitting corrosion of carbon steel applied to evaluating containers for nuclear waste disposal

G. P. Marsh[1], K.J. Taylor[2], A.H. Harker[3]

1. Strategic Studies Department, AEA Environment and Energy, AEA Technology, Harwell Laboratory
2. Applied Electrochemistry Department, AEA Industrial Technology, AEA Technology, Harwell Laboratory
3. Theoretical Studies Department, AEA Industrial Technology, AEA Technology, Harwell Laboratory

July 1991

THE KINETICS OF PITTING CORROSION OF CARBON STEEL
APPLIED TO EVALUATING CONTAINERS FOR NUCLEAR WASTE
DISPOSAL.

G P Marsh[1], K J Taylor[2], A H Harker[3]

1   Strategic Studies Department, AEA Environment
    and Energy, AEA Technology, Harwell Laboratory
2   Applied Electrochemistry Department, AEA
    Industrial Technology, AEA Technology, Harwell
    Laboratory
3   Theoretical Studies Department, AEA Industrial
    Technology, AEA Technology, Harwell Laboratory

July 1991

THE KINETICS OF PITTING CORROSION OF CARBON STEEL APPLIED TO EVALUATING CONTAINERS FOR NUCLEAR WASTE DISPOSAL

Final report 1991

*G.P. Marsh, **K.J. Taylor and +A.H. Harker

This report concerns a study which was conducted for SKB. The conclusions and viewpoints presented in the report are those of the authors and do not necessarily coincide with those of the client.

*Strategic Studies Department, AEA Environment and Energy

**Applied Electrochemistry Department, AEA Industrial Technology

+Theoretical Studies Department, AEA Industrial Technology

The Kinetics of Pitting Corrosion of Carbon Steel
Applied to Evaluating Containers for Nuclear Waste Disposal

G.P. Marsh, K.J. Taylor and A.H. Harker

ABSTRACT

This is the final summary report on a project, funded by SKB, investigating the pitting corrosion of carbon steel containers for high level nuclear waste or spent reactor fuel under granite disposal conditions. The study has covered a statistically based experimental programme to establish the pit growth kinetics, and a modelling study to determine the maximum pitting period subsequent to repository closure. It is shown that the rate of pit propagation is slower than that suggested by earlier work and that the maximum pitting period is only a small fraction of the target container life of 1000 years. An illustrative example of the methodology for estimating the corrosion allowance needed to prevent pit penetration is given. This could be applied to specific repository conditions as defined by SKB. Finally some limited recommendations are made for further studies to test and validate the methodology.

CONTENTS

TABLES

FIGURES

1. INTRODUCTION

Between 1980 and 1985 Harwell conducted a programme, which was jointly sponsored by the UK-DoE and the CEC, to investigate the corrosion behaviour of carbon steel containers for the disposal of High Level Nuclear Waste (HLW) in a granitic repository[1]. This study showed that, with certain groundwater compositions, carbon steels could be subject to comparatively fast localised corrosion. Subsequent kinetic studies, using an extreme value statistical approach to make allowance for the difference between specimen areas and the larger surface areas of waste containers, showed that at 90°C the most probable maximum pit depth increased with time in years according to the expression

$$P = 8.35\,T^{0.46}\ (\text{mm})\ . \qquad\qquad (1.1)$$

This inferred that a metal thickness of 200 mm would be needed to prevent container penetration by pitting over a 1000 year period. Clearly such a large corrosion allowance, although feasible, will complicate container design, manufacture and handling in the repository. It is therefore important to be confident of the accuracy of the equation (1.1).

In a second programme for the UK-DoE/CEC the pit growth study was extended to a maximum test period of 30,000h[2]. Using this extended data set the empirical equation for the increase in maximum probable pit depth with time was revised to

$$P = 7.01\,T^{0.42}\ (\text{mm}) \qquad\qquad (1.2)$$

which still implies a corrosion allowance of 128 mm to prevent pit penetration over 1000 years.

In the final report of the first UK-DoE/CEC project it was concluded that equation (1.1) was probably over conservative for the following reasons:

(a)   The particular form of extreme value statistical analysis used in the study assumed that the overall pit depth distribution fitted an unlimited distribution function. In reality mass transport and migration restrictions within pits are likely to set an upper limit to the depth of penetration attainable at any one time.

1

(b)   The equation is based on the results of experiments lasting only a few thousand hours in which the maximum pit depth was ~3.5 mm. The extrapolation of such short term shallow pit data to long term deep pitting assumes that the same pits will continue to propagate. It is at least equally likely, however, that restrictions on mass transport and ion migration will cause periodic stifling of deep pits, and subsequent initiation of new pits at the outer metal surface.

(c)   It may be unrealistic to assume pitting will occur during the full life required from the containers. Localised corrosion is only possible in environments which are sufficiently oxidising to stabilise a protective oxide film on the bulk of the metal surface. This condition may not prevail in a repository for 1000 years.

(d)   The pit growth experiments were conducted at a constant electrochemical potential, which is equivalent, under repository conditions, to an unlimited supply of cathodic reactant (e.g. Oxygen). In practice the supply of reactant is likely to be limited by diffusion.

In 1986 SKB contracted Harwell to advance the assessment of localised corrosion of carbon steel containers in granitic environments, through a research programme which addressed the issues described above. This is the final report on this programme, which, for clarity of presentation, has been divided into four main sections.

(i)   Statistical analysis of pit growth data.
(ii)   Stability and growth of deep pits.
(iii)   Aeration period at the container/backfill interface.
(iv)   Re-appraisal of the corrosion allowance for pitting.

2.   STATISTICAL ANALYSIS OF PIT GROWTH

The depths of pits formed in carbon steel after a fixed exposure period are not all the same, but have a statistical distribution. This is due to three factors:

(a)   Pits initiate at different times.
(b)   Some pits may cease to propagate before the end of the exposure period.
(c)   Pit growth rates may also be variable.

2

Because pit depths are statistically distributed the probability of finding a pit of depth greater than x increases with the surface area of metal exposed. This factor must be taken into account when predicting the maximum depth of pitting in HLW containers from tests with comparatively small surface area specimens.

In the original UK-DoE/CEC programme pit depth data were adjusted to take account of surface area using Type I Extreme Value Analysis[1], which assumes that the overall distribution of pit depths is unlimited. However, as mentioned in the introduction, intuitively it would be expected that there would be a physical upper limit to the pit depth attainable after any particular period, which will be fixed by charge and mass transport kinetics within the pit. It was also mentioned in the introduction that the experimental data obtained in the UK-DoE/CEC programmes were determined under constant electrochemical potential conditions, which may be more severe than those pertaining in a repository.

In view of the above factors this part of the SKB programme had the following objectives:

(a) to develop and appraise alternative methods of statistical analysis.

(b) to investigate the kinetics of pit growth under polarisation conditions more representative of those pertaining in a repository.

(c) to widen the experimental study to investigate the influence of temperature, solution concentration and welding on pit growth.

2.1 Development of Statistical Methods
2.1.1 General distribution functions

The distribution of any continuous statistical variable x can generally be described by a cumulative distribution function F(x). This gives the probability that a single sample from the population will have a value less than or equal to x. The most commonly used distribution function is the Gaussian or Normal Distribution, but other useful distributions include Log-Normal, Poisson, Weibull, Binomial and Cauchy.

In relation to pitting corrosion two distribution functions are potentially applicable. The first is the exponential function:

$$F(x) = 1 - \exp[-b(x - x_0)] \ . \tag{2.1}$$

This is a particular form of the Weibull Distribution with a shape parameter C=1; b is the scale parameter characterising the spread of the distribution and x_0 is a location parameter. It is the distribution function most commonly used to analyse pit depth data, either in its general form (2.1) or through the Type 1 Extreme Value distribution function, which is derived from it[3].

The second distribution function is the generalised limited function:

$$F(x) = 1 - \left[\frac{w-x}{w-u}\right]^k \qquad (2.2)$$

where w is the upper limiting pit depth, u a location parameter and k a shape parameter.

The cumulative probability $F(x)$ can be calculated from experimental measurements of all the pit depths in a specimen using the expression

$$F(x) = \left[\frac{n}{N+1}\right] \qquad (2.3)$$

where n is the number of pits in the specimen of depth $\leq x$ and N is the total number of pits in the specimen. By fitting equation 2.1 and 2.2 to the experimental results the distribution function which most closely represents the pit depth distribution in the metal can be identified.

Once established, the distribution function can be used to calculate the probability of all pits in a metal surface being $\leq x$. For example if there are N pits in a metal surface of area a, the probability that they will all be $\leq x$ is $F(x)^N$. Similarly for another area A the probability will be $F(x)^{\frac{NA}{a}}$, where N/a is the pit density. With regard to waste containers, the important factor is the probability that no pits will have a depth $> x$ (i.e. $P(x)$). This will be given by

$$P(x) = 1 - F(x)^{\frac{NA}{a}} \qquad (2.4)$$

for a container of surface area A, when N is the total number of pits in a specimen area 'a' (i.e. the experimental estimate of pit density). This equation can be used to estimate the corrosion allowance x, needed to reduce the probability of pit penetration to some predetermined level $P(x)$.

This method of analysis was applied to the data from the UK-DoE/CEC project[4] as part of the SKB programme. Surprisingly it was found that in general the data correlated best with the unlimited exponential distribution function. However, it was noted that the correlation was heavily dependent on the last 4-5 high pit depth data points, which were the ones having the greatest scatter. It was concluded, therefore, that a tendency for a 'tail off' in the data, towards a limiting pit depth, might be more detectable if the results were extended to lower probabilities by using larger specimens (i.e. a larger sample of pit population). It was also found in conducting the UK-DoE/CEC study that the measurement of the total distribution of pit depths was both slow and tedious and also prone to considerable error. The latter arose because the pits tended to overlap such that it became increasingly difficult to identify individual pits as the exposure time grew longer. For these reasons it was decided to concentrate on an Extreme Value approach to the appraisal of pitting in the remainder of the present study.

2.1.2 Extreme value distribution functions

For a number of specimens of equal area the deepest pit in each will have a cumulative distribution function $\phi(x)$ which originates from the overall distribution function $F(x)$. Three extreme value distribution functions have been developed which are usually designated Types I, II and III[3]. Type I is an unlimited function, which is derived from the overall exponential distribution function (2.1), and has the form:

$$\phi(x)_I = \exp\left[-\exp[-b(x - U_N)]\right] \tag{2.5}$$

where $\phi(x)_I$ is the cumulative probability that the deepest pit in a metal sample containing N pits has a depth $\leq x$. U_N is the characteristic deepest pit and b is the same scale parameter as for the overall distribution.

The Type II distribution is applicable to variants which are limited at the lower end of their range (e.g. climatic variables such as winter temperature). Such a distribution is not applicable to pitting. Conversely the Type III distribution is limited at the upper end of the range, and is derived from the overall limited distribution function (2.2). It has the form

$$\phi(x)_{III} = \exp\left[-\left(\frac{w - x}{w - u}\right)^k\right] \tag{2.6}$$

5

where w is the maximum or limiting pit depth, u is a scale parameter, which determines the location of the distribution, and k determines the spread or shape of the distribution.

In addition to the three functions discussed above a Generalised Extreme Value (GEV) distribution function has been developed by Jenkinson[5] which subsumes all three types into a single formula. In this the sign of the shape parameter β indexes the type of distribution (i.e. unlimited Type I β = O; Type II β < O; Type III β > O).

$$\phi(x)_{III} = \exp\left[-\left(\frac{w-x}{w-u}\right)^k \right] \qquad (2.7)$$

where β is a shape parameter, d a location parameter and α a scale parameter. When the function is limited at the upper bound, the maximum pit depth is given by:

$$w = d + \alpha/\beta \qquad (2.8)$$

The applicability of this function, along with the Type I and III distributions, has been investigated in this work.

The extreme value distribution function can be estimated experimentally by measuring the deepest pit in each of m specimens of equal surface area, or m equal areas in a single specimen, and is given by

$$\phi(x) = \frac{\ell}{m+1} \qquad (2.9)$$

where ℓ is the ℓth largest of the m maximum pit depths. It should be noted that implicit in this calculation is the assumption that the pit density is the same in all specimens. This is important because the extreme value functions are derived from the basic principle that $\phi(x) = F(x)^N$.

The advantage of the extreme value approach is that it only requires the maximum pit depths to be measured. This is much less laborious than having to measure all pits, and, more importantly, it avoids the errors involved in identifying and counting all pits.

As explained at the beginning $\phi(x)$ gives the cumulative probability that x will be the deepest pit in a single specimen. The probability that x will be the deepest pit in R

specimens, each of the same area and hence assumed to contain the same number of pits N, is therefore $\phi(x)^R$. If the experimental programme is conducted with specimens of area 'a' and the containers have an area A, then the probability that x will be the deepest pit in a container will be given by $\phi(x)^{A/a}$. Also the probability of a pit developing which is deeper than x is:

$$P(x) = 1 - \phi(x)^{A/a} \qquad (2.10)$$

2.1.3 Application of extreme value analysis to UK-DoE/CEC results

On completion of the second UK-DoE/CEC programme, which extended the pit growth studies to 30,000h, the pit depth data were analysed using both the Type I and Type III extreme value functions. The results of this study are listed in Table 1, which shows that only the data from the tests lasting 17500 and 30,000h correlated more closely with the limited distribution (Type III). Unfortunately when the work was done the only method available for fitting the results to the distribution functions was by first linearising them by taking logs, and then applying linear least squares regression analysis. Furthermore the GEV function was not available at that time.

Recently a non-linear least squares fitting programme has been developed for the Type I and Type III and GEV functions, which has enabled the UK-DoE/CEC data to be re-analysed. With this programme the quality of fit is measured by the value of chi-squared; the smaller the value the better the fit. Results of this new analysis are listed in Table 2.

With this new approach there is little difference in the correlation, as given by chi-squared, up to exposures of 10,000h. However, the data from the 17,500 and 30,000h tests have a better correlation with the Type III and GEV functions. Both of these functions yielded virtually the same limiting pit depth for the two exposure periods. This is to be expected since the GEV function should produce the same distribution function as whichever of the specific functions fits the data most closely. The actual limiting pit depths are slightly larger than estimated by the earlier analysis (Table 1).

To explore the quality of correlation more fully the upper and lower 90% confidence limits for the limiting pit depth x were calculated for the three distribution functions. These and the lines representing the best fit are plotted in figures 1 and 2 for the Type I and GEV functions. Type III is almost identical to the GEV and has not been reproduced here. It will be noted that the confidence limits are narrower for the unlimited distribution than for the GEV (or Type III) function. In fact for some data the

7

confidence limits for GEV lie outside the range used for the graph. This indicates that the unlimited distribution gives the best representation of the distribution of pit depths. The reason for the favourable showing of the Type I distribution is that it has only two fitting parameters (b and U_N) whereas the other distributions have three. Therefore, although the latter may give a marginally better correlation as measured by chi-squared there is greater total error in the derivation of the fitting parameters.

2.2 Experimental Studies of Pit Growth
2.2.1 Experimental procedures
In the UK-DoE/CEC programme, referred to previously[1], an experimental technique was developed for measuring pit depth distributions after fixed exposure periods. The apparatus consisted of a threaded cylindrical specimen of 42mm diameter, which was screwed into the base of a tubular PTFE vessel so that 8 cm^2 of the specimen was exposed to the electrolyte. These assemblies were heated in an oil bath, and the specimens were subject to potentiostatic control. After the required exposure period the distribution of pit depth was measured by an incremental grinding procedure involving successive removal of 0.05 mm of metal and manual counting of the number of pits remaining. Experiments were run in groups of 5 so that the effective sampling area was 40 cm^2. This also enabled the deepest pit depths recorded in each specimen to be used for an extreme-value statistical analysis.

It was explained in the Introduction and Section 2.1.1 that this experimental method had two disadvantages

(i)   The sample area of 40 cm^2 was small.

(ii)   The potentiostatic (constant electrode potential) control applied to the specimens simulates a situation in which the corrosion process is not limited by the supply of cathodic reactant (O_2 in the case of pitting), whereas in a repository the supply will be limited by diffusion through the backfill.

Consequently in the present study larger plate specimens of 440 cm^2 area were used. Also the specimens were subject to constant current polarisation, which is equivalent to a constant flux of cathodic reactant reaching the metal surface, and therefore is a reasonable simulation of the steady state diffusion of oxygen through a backfill to the container surface. The control current selected was 5μA cm^{-2}, which is about the maximum current which could be supported by the steady state diffusion of oxygen

8

through a 0.5m thickness of backfill (D = 10^{-10} m^2 sec^{-1}) from a tunnel flooded with water containing 8×10^{-3} mole dm^{-3} of oxygen.

These tests were undertaken with rectangular plates of carbon steel (Grade BS4360 43A) of composition 0.2%C, 0.08%Si, 0.67%Mn, 0.038%S and 0.01%P. The plates, with their edges and lower faces screened with lacquer, were placed in an upward facing orientation in polypropylene lined tanks containing 7 litres of electrolyte. The test solution used was the same 0.1M $NaHCO_3$ + 1000 ppm Cl⁻ solution used in the UK-DoE/CEC study in order to facilitate comparison between the results.

In these tests the incremental grinding procedure was only used to determine extreme value pit depth data. This was done by dividing the specimen surface into 4 cm^2 sections by means of a transparent grid overlay. After the successive removal of 0.025 mm thicknesses of metal each grid section was scanned to determine the depth at which all signs of corrosion had disappeared. In this way it was possible to obtain a sample of up to 110 maximum (i.e. extreme value) pit depths.

2.2.2 Results of tests at ambient temperature and 90°C

Tests in the standard 0.1M $NaHCO_3$ + 1000 ppm Cl⁻ solution at ambient temperature and 90°C were conducted for periods ranging from 1000 to 26000 hours. The absolute maximum pit depths observed in these tests together with their aspect ratios (i.e. ratio of maximum pit depth to uniform corrosion depth produced by a current of 5 μA cm^{-2}) are listed in Table 3. Surprisingly the pit depths were greater at ambient temperature than 90°C. It is also apparent that the rate of pit growth declined with time, and as a consequence so too did the aspect ratio.

Once again the correlation as measured by chi-squared (Tables 4 and 5) is inconclusive only showing a marginally better fit for some data sets for the Type III and GEV functions. To further investigate the quality of fit of these equations to the experimental data the 90% confidence limits were estimated and these are plotted together with the best fit values for the Type I and GEV functions in figures 3 and 4 for the 90°C results . In common with the results reported in the previous section these plots show a narrower range of uncertainty with the Type I distribution. Corresponding results for the ambient temperature tests show the same characteristics and the 90% confidence limits were once again narrower for the Type I distribution.

The Type I distribution function has been used in accordance with equation 2.10 to estimate the pit depth having a 0.1 probability of being exceeded in a canister area of

$4m^2$. The results for each test period used in the experimental programme are presented in figure 5 for both 25 and 90°C. Non-linear regression analysis of these data yielded the following empirical growth equations:-

$$(25°C) \quad P = 2.89T^{0.34} \text{ (mm)} \qquad\qquad (2.11)$$

$$(90°C) \quad P = 3.08T^{0.22} \text{ (mm)} \qquad\qquad (2.12)$$

A notable feature is that the time exponent is now distinctly smaller, and consequently the corrosion allowances given by these equations for a 1000 year period, at 31 mm and 14 mm respectively, are substantially smaller than that given by the same non-linear analysis of the DoE/CEC data which yielded the results plotted in figure 6. These fit the empirical growth equation,

$$P = 7.31T^{0.53} \text{ (mm)} \qquad\qquad (2.13)$$

which gives a corrosion allowance of 280 mm after 1000 years. This markedly different outcome is probably linked to the nature of the tests in that the DoE/CEC ones were conducted at constant potential whereas the present tests were under constant current conditions.

As discussed in Section 2.2.1, in the tests under potentiostatic control pit growth would not have been limited by the supply of reaction current whereas in the constant current situation current supplied to individual pits will be limited as they grow larger and additional pits initiate. The series of photographs in figure 7, showing the development of localised corrosion with increasing test period in the 90°C tests, illustrate that sites do indeed spread and gradually cover an increasing proportion of the metal surface up to about 12,000 hours. Beyond this time the proportion of the surface attacked appears to be fairly similar. Specimens tested at ambient temperature exhibit the same behaviour.

2.2.3 Results of tests on welded specimens at 90°C

These tests were undertaken with plate specimens cut from a 10 mm thick block of carbon steel containing a full penetration autogeneous electron beam weld (supplied by the Welding Institute, Cambridge, UK). The steel was of BS4360-43A specification with the composition 0.30%C, 0.28%Si, 0.90%Mn, 0.06%S and 0.01%P. Separate analysis of the weld metal yielded the composition 0.27%C, 0.26%Si, 0.86%Mn, 0.006%S and 0.009%P. These specimens had an exposed surface area of 224 cm^2 with the weld passing through their centres.

The specimens were tested in 0.1M NaHCO$_3$ + 1000 ppm Cl$^-$ at 90°C under a constant polarisation current of 5µA cm^{-2} at 90°C for periods ranging from 1025 to 15,096h. Visual examination revealed no preferential corrosion of the weld or its heat affected zone (figure 8), and in fact the maximum pit depths in all the tests were found in the parent material. The absolute maximum pit depths observed, and their associated aspect ratios are listed in Table 3. Figure 8 also shows that the area of metal surface subject to corrosion increases progressively with test period. Results of the statistical analysis of the pit size distribution data from these tests are presented in Table 6. The Type III and GEV distribution functions clearly have a better quality of fit compared to the Type I than was apparent with the previous data sets. However it is noticeable that the limiting pit depths estimated from these functions did not show the steady increase with exposure time that would be expected. Confidence limits for the three functions were not calculated in this case, but given the observations reported for previous data sets and the anomalous trend in limiting pit depths referred to it was decided to remain with the Type I function in analysing these results. The pit depths with a probability of 0.1 of being exceeded in a container of 4 m^2 area are shown in figure 9. It was not possible to derive an empirical rate equation in this instance because of the scatter of data which came from fewer tests over a limited time scale.

2.2.4 Results of tests in oxygenated solution

These tests were undertaken to demonstrate that pitting can be produced in 0.1M NaHCO$_3$ + 1000 ppm Cl$^-$ solution without external polarisation, and to compare the pitting kinetics with those observed in the constant current experiments (Section 2.2.2 and 2.2.3). The experiments were conducted according to the procedure described in Section 2.2.1 except that oxygen was continuously bubbled into the electrolyte, which was heated to 50° C.

Results from the statistical analysis of the data from these experiments are listed in Table 7. Once again the quality of fit, as measured by chi-squared, is inconclusive in pointing to any one of the distribution functions giving a better fit on a consistent basis. For this reason the Type I function has been used to analyse the results which are plotted in figure 10. These yielded the following empirical rate equation

$$P = 4.74T^{0.35} \qquad (2.14)$$

The limiting pit depths given by the Type III distribution are generally greater than those estimated for equivalent exposure periods with the galvanostatically controlled

experiments. This is probably because the oxygen flux to the specimens in these tests is equivalent to a greater cathode current than the $5\mu A$ cm^{-2} used in the constant current tests. This view is supported by the observation that the electrode potentials, particularly in the longer term oxygenated tests, were on a rising path whereas the potentials tended to fall with time in the constant current experiments.

2.2.5 Discussion

Considering first the electrochemically controlled experiments, two sets of data have been presented herein, namely those from potentiostatically controlled and constant current tests. It is important to be clear what is being measured in these tests. With potentiostatic control the corrosion processes occuring are not limited in their form or rate of propagation by the maximum balancing cathode reaction current; essentially whatever the magnitude of the corrosion current this will be sustained by the electronic controller. Under these conditions pit growth should not be constrained by external polarisation, and therefore the rates measured will only be limited by the charge and mass transport processes occuring within the pits themselves. In contrast under galvanostatic control, in which the current supplied to sustain corrosion is fixed, pitting may be limited either by external polarisation or internal mass and charge transport, whichever is the slowest step. At high current densities it is probable that the internal pitting processes will remain limiting. However, at the low currents used in the present work, it is probable that, particularly over long test periods, the current will not be sufficient to maintain the growth of all pits in the specimen. When this situation develops some pits must cease to propagate, and if these happen to be the larger pits this will be manifested in the experimental results as an apparently slower rate of pit growth.

Turning to the chemically controlled or oxygenated tests it will be apparent that these could show behaviour equivalent to either potentiostatic or constant current control depending on the the corrosion behaviour of the metal. At low corrosion rates (e.g. when the metal is mainly passive with a few pits) the oxygen supply will be in excess and the behaviour will be equivalent to potentiostatic control. However, if a lot of corrosion is occuring and/or the oxygen supply is limited, then the conditions will be analogous to constant current control.

The new statistical analysis indicated a closer correlation for most data sets with a limited (Type III or GEV) distribution, ostensibly supporting the hypothesis described in the Introduction, that there must be a physical limit to the rate of pit growth. However, the improved correlation was not sufficient to be conclusive and further

investigation showed the improvement to be due to the limiting distributions having three fitting parameters compared to the two of with the unlimited function. It was also found that the confidence limits on the maximum pit depths calculated with the distribution functions were generally less with unlimited function. Because of this unequivocal position it has been necessary to abandon the original objective of establishing upper limits to pit growth, and to revert to analysis based upon the unlimited Type I distribution.

With this background the implications of the experimental results can be examined. Commencing with the UK-DoE/CEC data, which were reanalysed in section 2.1.3 with the non-linear least squares fitting routine, the empirical growth law has been revised from $P = 7.01T^{0.42}$ (Eqn. 1.2) to:

$$P = 7.31T^{0.53} \tag{2.15}$$

This law must represent the growth of pits limited only by internal charge and mass transport processes, without any external polarisation constraints. Because the growth law represents internal growth limits it should not be too sensitive to external environment composition changes, so long as the environment still has the critical balance of activating and passivating species, which is a pre-requisite for pitting. The equation should, therefore, be applicable for making a first order 'worst case' evaluation of pit propagation over a wide range of repository environments. The one qualification on this that there is evidence that this growth law may increase with the applied electrode potential[6]. However, the potential of -200mV(SCE) used in the tests is at the high end of the range likely to be attained in practice, and therefore should form a sound basis for a first order 'worst case' evaluation.

With regard to the constant current experiments, it has been shown that these too yield data with the narrowest confidence limits when fitted to a Type I. However the growth laws for the maximum probable pit depths derived from these pit depth data sets have a smaller time exponent and as a consequence predict significantly smaller corrosion allowances. If it could be demonstrated that these constant current (limited polarisation) conditions also apply in practice to repository conditions, considerable benefit could be derived from a substantially reduced corrosion allowance. The establishment of such polarisation limited growth conditions will depend on the rate of supply of oxidants to the surface and their rate of consumption. In particular the rate of oxygen consumption will depend on both the number of pits produced on a container and the rate of passive corrosion, both of which may vary depending upon the environmental conditions in the

repository, and for that matter for different locations within the repository. This question is explored further in section 4.

To further explore the validity of using constant current in pit growth data comparisons have been made with the long term field experiments conducted by Romanoff[7], in which thousands of specimens were buried in a wide range of soil types at many test locations. The deepest pits observed by Romanoff in tubular test pieces of a similar carbon steel to the one used in our experiments are presented as a scatter band in figure 11. The results from our tests have been extrapolated to the same surface area as Romanoff's specimens and the resulting empirical rate equations used to predict the deepest pits, with a 0.1 probability of being exceeded, as a function of exposure period. These are shown as solid lines in figure 11. It is evident that the constant current results relate more closely to the field test data than do the UK-DoE/CEC constant potential data. This further reinforces the view that galvanostatic controlled experiments are more relevant to practical situations.

3. STABILITY AND GROWTH OF DEEP PITS

The original intention in this part of the study was to investigate both the perpendicular and lateral propagation rates of deep artificial pits. These were to be produced by drilling holes into a block of carbon steel. In the event a very similar study was published by Beavers and Thompson[8] before this work could be started. Their work demonstrated the strong tendency of pits in carbon steel to spread laterally. In fact this has such significance in the overall analysis of pitting that a short summary is given below.

3.1 Results of Beavers and Thompson

Most mechanistic models for pit propagation assume that the pit walls are unreactive. In the majority of these models the pit propagation rate is controlled by the transport of corrosion products out of the pit. Many experimental studies performed in conjunction with such modelling studies use potential or current control with auxiliary electrodes. This approach may artificially accelerate pit propagation by promoting mass transport control as opposed to activation control.

In Beavers' and Thompson's tests the free corrosion pit propagation behaviour of reactive wall and non-reactive wall pits was compared. Their results demonstrate that these are significantly different.

14

For non-reactive wall geometry relatively high propagation rates occur for deep pits because of the coupling effect of the external exposed surface.

With reactive wall pits the high rates of attack are confined to the region near the pit mouth because the high potential drop within the solution in this region effectively minimises polarisation of the deeper parts of the pit. This creates a condition in which the rate of propagation within deep pits is controlled by the electrode kinetics within the pits.

Thus pitting models based on non-reactive walls will overestimate pit propagation rates. In addition these models predict much lower diameter:depth ratios for (i.e.deeper pits) than are likely to occur in service.

The results of Beavers study are consistent with the shallow pit geometries generally observed on buried carbon steel structures.

3.2   Pit Profile Measurements

Rather than repeat the above investigation it was decided to make an alternative check on the tendency for pits in carbon steel to spread laterally by measuring the profiles of naturally grown pits produced in the experimental programmes. This was done by measuring the diameter of selected (deeper) pits between incremental grinding stages in the pit depth measurement process.

Figures 12 and 13[9] show the results of this work for tests under constant current and potentiostatic conditions respectively. In both cases it is apparent that the pits appear to have diameter:depth ratios of 4-6 supporting the view that pits in carbon steel have a tendency to spread laterally faster than they increase in depth.

4.   AERATION PERIOD AT THE CONTAINER-BACKFILL INTERFACE

It is well established that pitting corrosion of the type considered herein, occurs by an occluded cell process which is driven by a potential gradient between the anode (pit) site and the external cathodic surface. The mechanistic basis for this conclusion, and the environmental and electrochemical requirements to maintain the necessary potential gradient, have been re-examined as part of this project, to determine if they offer a basis for estimating a maximum pitting period under repository conditions. A full description of this analysis and its conclusions, have been published in two reports[10,11], and therefore only a short summary is given here.

4.1 Basis of Analysis

Consideration of the mechanism of pitting corrosion in carbon steel shows that the process will only occur if the external metal surface is passive (i.e. protected by an oxide layer). Furthermore, the requirement for maintaining such a passive state is that the rate of reduction of oxidising species on the metal surface must be sufficient to balance the rate of oxidation of metal atoms, due to slow corrosion through the passive film. Under diffusion controlled mass transport conditions this condition can be represented by the equation

$$I_{CORR} \leq \sum_{i-1}^{l} n_i F J_i \qquad (4.1)$$

where I_{CORR} is the passive corrosion current density, F Faraday's constant, n_i and J_i the valence and flux of the oxidising species, and the summation covers the l oxidising species in the system. The equation assumes that the rate of reduction of the oxidising species is controlled by their rate of transport to the metal surface.

The time at which this inequality ceases to be satisfied marks the time at which localised corrosion ceases to be possible.

Solutions to this inequality have been calculated using a one dimensional mathematical model which examines the non-steady state diffusion of oxygen and oxidising radiolysis products to a carbon steel container surrounded by a bentonite backfilling. The model also considers the rate of production of oxidising radiolysis products, their recombination reaction chains and the decay of the γ-radiation dose with time.

The model has been used to make sensitivity studies of how the passivation time and hence pitting period is influenced by (a) the diffusion coefficients of the relevant species in the bentonite backfill (b) the initial radiation dose rate (c) the backfill thickness and (d) the rate of passive corrosion.

4.3 Diffusion Coefficient

The estimated variation of the passive period with corrosion current is illustrated in figure 14 for intrinsic diffusion coefficients for oxygen in a compacted bentonite backfilling of 2×10^{-11} and 1.2×10^{-10} m^2 sec^{-1}. [NB The intrinsic diffusion coefficients of the other species were scaled against these reference values by multiplying their known coefficients in water at 25°C by the ratio of the oxygen intrinsic value to the oxygen bulk water value]. These particular calculations were made for a

16

diffusion path length (backfill thickness) of 1.5 m. As would be expected, the passive period falls with increasing corrosion current reaching negligible times with currents exceeding 10^{-3} A m^{-2}.

At high currents the difference in passive period between the two diffusion coefficients is a factor of about 5 to 6, but it increases at lower currents. This is because the steady state diffusion flux with the higher diffusion coefficient is sufficient to support currents exceeding 1.7×10^{-4} A m^{-2} indefinitely, for the boundary conditions assumed in the model.

Figure 14 also contains a broken line showing the maximum passive period estimated from a mass balance calculation which assumes all oxygen within the repository is free to reach the container. Comparison shows that this is substantially greater than the estimates made by the model for the higher currents investigated in the study, but that the total quantity of oxygen available could become limiting at lower currents where mass transport is easily supported.

4.4 Radiation Dose Rate

The model has been used to investigate radiation dose rates of 10^2 and 10^3 Gy h^{-1}, and these results are included in figure 14. Radiation causes a small increase in the passive period, which is most significant at the higher corrosion currents. It is also noteworthy that the increase is predicted to be marginally greater with the lower of the two dose rates. The reason for this latter outcome is not immediately apparent and demands further investigation with the model. It should also be noted that the increase in passive period is substantially less than that predicted in the previous modelling study[12] in which the recombination reactions between radiolysis products were neglected.

4.5 Backfill Thickness

The influence of backfill thickness on passive period was investigated by running the model for thicknesses of 1, 1.5 and 2.0 m, assuming a passive corrosion rate of 5×10^{-4} A m^{-2} and a radiation dose rate of 100 Gy h^{-1}. With the higher diffusion coefficient of 1.2×10^{-10} m^2 sec^{-1} (intrinsic value for oxygen) the passive period declined from 106 years through 73 to 63 years with increasing backfill thickness. However, with the lower diffusion coefficient of 2×10^{-11} m^2 sec^{-1}, with which the inter-change of species with the tunnel was much reduced, the effect of backfill thickness was negligible.

4.6 Discussion

The primary purpose of this study was to develop a mechanistically based approach for estimating the maximum period for localised corrosion of waste containers, and hence the point of transition to a uniform mode of degradation. In so doing, the study has highlighted the sensitivity of this transition to the diffusivity of the backfill and to the passive corrosion rate of the carbon steel containers. This in turn gives a clear pointer to the direction of future experimental studies.

Although the model is essentially complete its application should strictly be limited to 25°C, which is the temperature at which the necessary radiation chemistry data were obtained. However, these rate constants are so fast that the reactions probably do not limit the system in any way, in which case behaviour at other temperatures may be gauged with appropriate combinations of diffusion coefficient and passive corrosion current.

To illustrate the benefit of this analytical approach the maximum period for localised corrosion will be estimated for a radiation dose rate of 10^2 Gy h^{-1} (the initial surface dose from a carbon steel container of 100 mm wall thickness) at 25 and 90°C. At the lower temperature the diffusion coefficient will be 2×10^{-11} m^2 sec^{-1}[13] and the passive corrosion current about 5×10^{-4} A m^{-2}. The latter is probably a conservative estimate because the literature reports values of $\sim 10^{-2}$ A m^{-2} for pure HCO_3^- and CO_3^{2-} solutions[14,15]. For these values figure 14 gives a maximum passive period (localised corrosion feasible) of 10 years for a backfill thickness of 1.5m. At 90°C the diffusion coefficient increases to 1.2×10^{-10} m^{2}sec^{-1}[13], and, although data are not available, it is probable the corrosion rate also rises. For the purpose of this example it is assumed to be 10^{-3} m^{2}sec^{-1}. For these values figure 14 gives a passive period of about 14 years (backfill 1.5 m). Clearly these times are very small compared to the lifetime required of the containers or the maximum passivation time calculated by neglecting mass transport, which was described earlier.

5. RE-APPRAISAL OF CORROSION ALLOWANCE FOR PITTING

The estimation of a suitable corrosion allowance to prevent container penetration by pitting requires data on the rate of pit growth and on the duration of pitting attack. Both of these factors have been investigated in this programme. Dealing with them in turn, the present work has highlighted a significant difference in the growth kinetics of pits depending on whether the metal is subject to constant current or constant potential polarisation. It has been argued that constant current polarisation is most relevant to repository disposal conditions, and this view has been supported by comparison of the

two sets of growth kinetics with results from long term field experiments in the USA[7]. Since, as is shown below, the choice of growth kinetics has a significant influence on the size of the corrosion allowance, it is recommended that further support for the choice of experimental conditions is sought through comparison with other field test and archaeological evidence.

Analysis of the aeration period of the repository has yielded estimates of 10 years for 25°C increasing to 16 years at 90°C. These values are considerably lower than the first set of estimates derived from this approach[12], which is because the earlier work neglected the recombination reactions of the radiolysis products, and hence over-estimated their oxidising effect. These estimates also have a significant influence on the size of the corrosion allowance, consequently it is recommended that consideration is given to the execution of tests to validate the model's predictions.

Actual calculation of the pitting corrosion allowance for an SKB repository and container design from the data reported here requires the specification of a range of parameters. With regard to the pit growth analysis the repository temperature is needed along with the probability level for pit penetration. In the present case a 0.1 or 10% probability was used for illustrative purposes. Similarly for the passivation or pitting period the estimation is sensitive to the expected repository temperature, the diffusion coefficient of the backfill and the backfill thickness. For this reason the estimation given below is only for the purpose of example, although the data and modelling capability exists to examine any set of specified conditions.

The faster of the two main growth laws established in the present study was for 25°C:

$$P = 2.89T^{0.34} \text{ (mm)} \tag{2.11}$$

The longer of the two pitting periods was 16 years for 90°C. Combining these yields on pit depth with a 0.1 probability of being exceeded equal to 5.6 mm. The use of this value as a corrosion allowance would neglect the statistical uncertainties in first estimating the pit depths with a 0.1 probability of being exceeded for each experimental period, and secondly the regression analysis of these pit depths to establish a growth law. This has not been done in the present study due to time limitations, although the data are available to do it. However, a crude estimation can be made from figure 3, which shows that the upper 90% confidence limits on the estimated maximum pit depths were about a factor of two greater than the median value. Applying this rule of

19

thumb to the corrosion allowance suggests a thickness of about 15 mm would be more realistic. It should be stressed again, however, that this is only an illustrative figure.

6. CONCLUSION

This project has been directed at investigating a number of aspects of the pitting corrosion of carbon steels under conditions relevant to the granitic disposal of heat generating nuclear waste or spent reactor fuel. The aim in so doing was to establish a methodology for estimating the corrosion allowance needed to prevent pit penetration of waste containers for at least 1000 years after emplacement. The main findings are:-

(i)   The statistical techniques and data fitting procedures available were not sufficiently discriminating to establish unequivocally that pit growth is bounded by an upper limiting pit depth which reflects the limit imposed by the kinetics of the pit propagation process. In fact it was found that the unlimited distribution function Type I offered the most accurate basis for analysing the experimental data.

(ii)   Pit growth laws have been determined to describe the propagation of pit depths having a 0.1 probability of being exceeded in a container of 4 m^2 area. These pit depths, established from tests conducted under constant current at 25 and 90°C, were significantly less than those for previous constant potential tests at 90°C. It has been argued that the constant current results are most relevant to repository conditions. It has also been recommended that further support for this view should be sought by comparing the results contained herein with other field test and archaelogical data.

(iii)   A model which analyses the duration of the passive period of waste containers under diffusion controlled mass transport conditions appropriate to a repository has been developed. This has shown that the passive period, which fixes the maximum period for pitting attack, is sensitive to temperature, backfill thickness, to passive corrosion rate of the containers, and the diffusion coefficients of oxidising species in the bentonite backfill. Input of reasonable estimates for these parameters yielded passive periods of the order of 10-16 years. In view of the importance of this finding in limiting the implications of pitting attack it is recommended that an experimental validation of the model should be undertaken.

(iv)   The pit growth data and modelling estimates of passive period can be combined
to give an estimate of the corrosion allowance needed to prevent pit penetration.
An illustrative example is given, and the data base exists to make more thorough
estimates in support of container designer for specified repository conditions.

ACKNOWLEDGEMENT

REFERENCES

1.   G.P. Marsh, I.D. Bland, K.J. Taylor, S.M. Sharland and P.W. Tasker , An Assessment of Carbon Steel Overpacks for Radioactive Waste Disposal, Report EUR-10437-EN, published by the Commission of the European Communities, 1986.

2.   G.P. Marsh, K.J. Taylor, S.M. Sharland and A.J. Diver, Corrosion of Carbon Steel Overpacks for the Geological Disposal of Radioactive Waste, Report DoE/RW/89/097, 1989.

3.   E.J. Gumble, Statistics of Extremes, published by Columbia University Press, New York/London, 1958.

4.   G.P. Marsh, K.J. Taylor and Z.J. Sooi, The Kinetics of Pitting Corrosion of Carbon Steel, SKB Technical Report 88-09.

5.   A.F. Jenkinson, 'Statistics of Extremes', World Met. Office, Technical Note, No. 98, 1969.

6.   K.J. Taylor, I.D. Bland and G.P. Marsh, Corrosion Studies on Containment Materials for Vitrified High Level Waste. AERE-G2970, 1984.

7.   M. Romanoff, Underground Corrosion, NBS Circ. 579, 1957.

8.   J.A. Beavers and N.G. Thompson, Effect of Pit Work Reactivity on Pit Propagation in Carbon Steel, Corrosion-NACE, 43 (3), p.185, 1987.

9.   B. Daniel, Corrosion Pitting of Carbon Steel in Alkaline Conditions, M.Phil. Thesis, University of Bath 1959.

10.   G.P. Marsh, J. Henshaw and W.G. Burns, Evaluating the General and Localised Corrosion of Carbon Steel Containers for Nuclear Waste Disposal. IAEA 641-TI-TC-703/4.

11.   G.P. Marsh, J. Henshaw and W.G. Burns. To be published.

12.   G.P. Marsh, S.M. Sharland and P.W. Tasker, An Approach for Evaluating the General and Localised Corrosion of Carbon Steel Containers for Nuclear Waste Disposal, MRS Symposium on the Scientific Basis for Nuclear Waste Management, Boston, December 1986.

13.   L. Ekbom, Copper as Canister Material for Unreprocessed Nuclear Waste - Evaluation with Respect to Corrosion, KBS-TR-90, Final Report 1978-03-31.

14.   J.G.N. Thomas, T.J. Nurse and R. Walker, Br.Corros.J., 5, 87-92, (March 1970).

15.   G.K. Glass, Corrosion Science, 26, No. 6, pp 441-454, (1986).

TABLE 1   SUMMARY OF THE RESULTS OF THE STATISTICAL
           ANALYSIS OF UK-DoE/CEC PROGRAMMES PIT
           GROWTH DATA (Ref. 2)

Test Period (h)	Type I			Type III	
	b (mm^{-1})	U_N (mm)	Correlation coefficient	Limiting Pit Depth (mm)	Correlation Coefficient
500	5.92	0.49	0.980	∞	-
1,000	3.73	0.47	0.950	∞	-
2,000	2.92	0.74	0.992	∞	-
3,000	2.45	1.02	0.984	∞	-
10,000	1.46	1.76	0.972	∞	-
17,000	1.45	1.51	0.969	3.7	0.987
30,000	1.15	4.18	0.969	7.5	0.989

TABLE 2   RESULTS OF THE STATISTICAL ANALYSIS ON THE UK-DoE/CEC PROGRAMMES PIT GROWTH DATA USING A NON-LINEAR LEAST SQUARES METHOD

Test Period (h)	Type 1			Type III				GEV				
	b (mm⁻¹)	U_N (mm)	(Chi)²	Limiting Pit Depth (w) (mm)	u (mm)	K	(Chi)²	Limiting Pit Depth (d) (mm)	α	β	d (mm)	(Chi)²
500	8.68	0.482	0.030	∞	0.482	∞	0.031	-	0.107	-0.213	0.479	0.027
1,000	5.16	0.525	0.012	∞	0.525	∞	0.012	-	0.192	-0.023	0.525	0.012
2,000	7.08	0.718	0.002	∞	0.718	∞	0.003	-	0.130	-0.170	0.715	0.001
3,000	2.85	1.004	0.009	2.752	1.019	4.523	0.005	2.752	0.383	0.221	1.019	0.005
10,000	2.14	1.743	0.012	∞	1.743	∞	0.012	-	0.458	-0.038	1.740	0.012
17,520	1.42	1.434	0.043	3.806	1.489	2,891	0.028	3.804	0.801	0.346	1.489	0.028
30,000	1.19	4.230	0.054	6.620	4.276	2.313	0.020	6.623	1.014	0.432	4.276	0.020

TABLE 3   ABSOLUTE MAXIMUM PIT DEPTHS AND ASPECT RATIOS MEASURED IN EXPERIMENTS IN 0.1M NaHCO$_3$ + 1000 ppm Cl⁻ SOLUTION AT AMBIENT TEMPERATURE AND 90°C

Exposure Period (h)	Ambient Temperature		90°C			Welded Specimens 90°C		
	Max. Pit Depth (mm)	Aspect Ratio	Exposure Period (h)	Max. Pit Depth (mm)	Aspect Ratio	Exposure Period (h)	Max. Pit Depth (mm)	Aspect Ratio
1,152	1.14	148.0	1,002	0.53	79.0	1,025	0.99	144.2
3,024	1.70	84.0	1,002	0.61	91.0	3,014	1.14	56.5
5,009	1.78	53.1	2,514	1.07	63.6	5,016	1.55	46.1
8,064	2.36	43.7	2,514	0.99	58.8	7,990	1.68	31.4
12,024	2.26	28.1	5,332	1.04	29.7	9,979	1.88	28.1
16,008	2.34	21.8	8,208	1.25	22.7	15,096	2.64	26.1
18,000	2.69	22.3	12,234	1.50	18.3			
22,005	2.08	14.1	16,048	1.35	12.6			
			22,008	1.58	10.7			
			26,016	1.9	10.90			

TABLE 4 RESULTS OF THE STATISTICAL ANALYSIS OF DATA OBTAINED FROM TESTS AT AMBIENT TEMPERATURE

Test Period (h)	Type I			Type III				GEV				
	b (mm^{-1})	U_N (mm)	(Chi)^2	Limiting Pit Depth (w) (mm)	u (mm)	K	(Chi)^2	Limiting Pit Depth (d) (mm)	α	β	d (mm)	(Chi)^2
1,152	21.86	0.138	0.011	0.577	0.139	9.102	0.010	1.136	0.051	0.051	0.136	0.012
3,024	16.63	0.213	0.046	∞	0.213	∞	0.046	-	0.059	-0.166	0.211	0.044
5,009	5.22	0.298	0.127	∞	0.298	∞	0.127	-	0.129	-0.608	0.282	0.029
8,064	3.48	0.663	0.010	∞	0.663	∞	0.010	-	0.270	-0.120	0.657	0.008
12,024	3.48	0.528	0.065	∞	0.529	∞	0.065	-	0.270	-0.200	0.516	0.052
16,008	2.53	0.613	0.020	7.565	0.617	17.083	0.019	7.515	0.407	-0.059	0.617	0.019
18,000	7.47	0.599	0.041	2.692	0.384	6.383	0.037	2.679	0.135	0.065	0.602	0.037
22,008	6.06	0.738	0.023	2.083	0.516	3.710	0.020	2.084	0.173	0.129	0.743	0.020

TABLE 5 RESULTS OF STATISTICAL ANALYSIS OF DATA OBTAINED FROM TESTS AT 90°C

Test Period (h)	Type I			Type III				GEV				
	b (mm⁻¹)	U_N (mm)	$(Chi)^2$	Limiting Pit Depth (w) (mm)	u (mm)	K	$(Chi)^2$	Limiting Pit Depth (d) (mm)	α	β	d (mm)	$(Chi)^2$
1,002	14.65	0.305	0.043	0.478	0.313	1.866	0.011	0.531	0.083	0.375	0.310	0.013
1,002	6.194	0.144	0.088	0.504	0.156	1.544	0.040	0.602	0.204	0.454	0.153	0.046
2,514	7.580	0.326	0.029	1.411	0.328	7.651	0.026	1.420	0.142	0.130	0.328	0.026
2,514	3.722	0.193	0.059	1.178	0.200	2.886	0.034	1.180	0.339	0.346	0.200	0.034
5,232	5.839	0.430	0.026	∞	0.430	∞	0.026	-	0.171	-0.008	0.430	0.026
8,208	5.306	0.411	0.061	∞	0.411	∞	0.060	-	0.148	-0.350	0.404	0.028
12,234	3.602	0.555	0.034	2.165	0.568	5.240	0.023	2.165	0.305	0.191	0.568	0.023
16,048	3.761	0.458	0.016	4.372	0.462	14.184	0.014	4.350	0.276	0.071	0.463	0.014
22,008	3.729	0.665	0.083	1.850	0.680	3.868	0.062	1.850	0.303	0.259	0.680	0.062
26,016	4.600	0.713	0.024	1.943	0.722	5.118	0.015	1.948	0.239	0.195	0.722	0.015

TABLE 6   RESULTS OF THE STATISTICAL ANALYSIS OF DATA OBTAINED FROM THE TESTS ON WELDED SPECIMENS

Test Period (h)	Type I			Type III				GEV				
	b (mm^{-1})	U_N (mm)	$(Chi)^2$	Limiting Pit Depth (w) (mm)	u (mm)	K	$(Chi)^2$	Limiting Pit Depth (d) (mm)	α	β	d (mm)	$(Chi)^2$
1,025	3.061	0.221	0.116	0.910	0.258	1.379	0.089	0.987	0.446	0.608	0.253	0.090
3,014	2.913	0.366	0.095	1.198	0.394	1.789	0.028	1.197	0.449	0.559	0.394	0.028
5,016	2.539	0.925	0.140	1.800	0.963	1.626	0.023	1.866	0.505	0.556	0.958	0.024
7,990	2.565	1.205	0.028	3.764	1.215	5.977	0.021	3.764	0.203	0.167	1.215	0.021
9,979	3.843	0.514	0.038	1.563	0.519	3.349	0.015	1,562	0.312	0.299	0.519	0.015
15,096	3.760	0.882	0.161	1.400	0.913	1.345	0.025	1,644	0.331	0.442	0.895	0.052

TABLE 7   RESULTS OF STATISTICAL ANALYSIS OF DATA OBTAINED FROM TESTS IN OXYGENATED SOLUTION AT 50°C

Test Period (h)	Type I			Type III				GEV				
	b (mm⁻¹)	U_N (mm)	(Chi)²	Limiting Pit Depth (w) (mm)	u (mm)	K	(Chi)²	Limiting Pit Depth (d) (mm)	α	β	d (mm)	(Chi)²
1,000	5.419	0.944	0.034	1.400	0.964	1.770	0.021	1.400	0.246	0.564	0.964	0.021
3,024	5.489	0.616	0.044	∞	0.616	∞	0.044	-	0.169	-0.109	0.615	0.041
5,064	4.510	0.736	0.036	1.664	0.748	3.597	0.008	1.662	0.254	0.278	0.748	0.008
11,064	2.208	1.093	0.034	4.151	1.109	6.247	0.025	4.153	0.487	0.160	1.109	0.025
31,128	2.252	1.582	0.040	∞	1.582	∞	0.039	-	0.405	-0.153	1.573	0.034

TABLE 8   G VALUES AND DIFFUSION COEFFICIENTS OF RADIOLYSIS PRODUCTS

	G (molecules per 100 eV)	D(*) (M^2 sec^{-1})
eq$^-$	2.7	4.5 x 10^{-9}
H$^+$	2.7	9.0 x 10^{-9}
G	0.61	7.0 x 10^{-9}
H$_2$	0.43	5.0 x 10^{-9}
OH	2.86	2.8 x 10^{-9}
H$_2$O$_2$	0.61	2.2 x 10^{-9}
HO2	0.03	2.0 x 10^{-9}

*Values for bulk water at 25°C

TABLE 9 REACTIONS OF RADIOLYSIS PRODUCTS

	Reaction		Rate Constant
1.	$e^-_{aq} + H_2O$	$\leftrightarrow H + {}^-OH$	$16/2.0 \times 10^4$
2.	$e^-_{aq} + H^+$	$\rightarrow H$	2.4×10^7
3.	$e^-_{aq} + OH$	$\rightarrow OH^-$	3.0×10^7
4.	$e^-_{aq} + H_2O_2$	$\rightarrow OH + OH^-$	1.3×10^7
5.	$e^-_{aq} + HO_2$	$\rightarrow HO^-_2$	2.0×10^7
6.	$e^-_{aq} + O_2$	$\rightarrow O^-_2$	1.9×10^7
7.	$(2H_2O) + 2e^-_{aq}$	$\rightarrow H_2 + 2OH^-$	5.0×10^6
8.	$(H_2O) + H + e^-_{aq}$	$\rightarrow H_2 + OH^-$	2.5×10^7
9.	$(H_2O) + e^-_{aq} + HO^-_2$	$\rightarrow OH + 2OH^-$	3.5×10^6
10.	$(H_2O) + e^-_{aq} + O^-_2$	$\rightarrow OH^- + HO^-_2$	1.8×10^5
11.	$OH + OH$	$\rightarrow H_2O_2$	4.5×10^6
12.	$OH + HO_2$	$\rightarrow O_2 + H_2O$	1.2×10^7
13.	$OH + O^-_2$	$\rightarrow O_2 + OH^-$	1.2×10^7
14.	$OH + H$	$\rightarrow H_2O$	2.0×10^7
15.	$OH + H_2$	$\rightarrow H + H_2O$	4.5×10^4
16.	$H + H$	$\rightarrow H_2$	4.5×10^4
17.	$+ H_2O_2$	$\rightarrow OH + H_2O$	1.0×10^7
18.	$+ HO_2$	$\rightarrow H_2O_2$	9.0×10^4
19.	$H + HO_2$	$\rightarrow H_2O_2$	2.0×10^7
20.	$H + O^-_2$	$\rightarrow HO^-_2$	2.0×10^7
21.	$H + O_2$	$\rightarrow HO_2$	1.9×10^7
22.	HO_2	$\leftrightarrow H^+ + O^-_2$	$8.5 \times 10^5/5.0 \times 10^7$
23.	$HO_2 + O^-_2$	$\rightarrow O_2 + HO^-_2$	1.5×10^4
24.	$HO_2 + HO_2$	$\rightarrow H_2O_2 + O_2$	2.7×10^3
25.	$H^+ + OH^-$	$\leftrightarrow H_2O$	$1.438 \times 10^8/2.6 \times 10^{-5}$
26.	$OH^- + H_2O_2$	$\rightarrow H_2O_2 + O_2$	$1.0 \times 10^5/1.022 \times 10^4$
27.	$H^+ + HO^-_2$	$\rightarrow H_2O_2$	2×10^7

1. Rate Constants are m^3 mol^{-1} sec^{-1} and sec^{-1} for second and first order reactions respectively.

2. Molecules in brackets are part of stoichiometry of the reaction but are not includedin the rate equations.
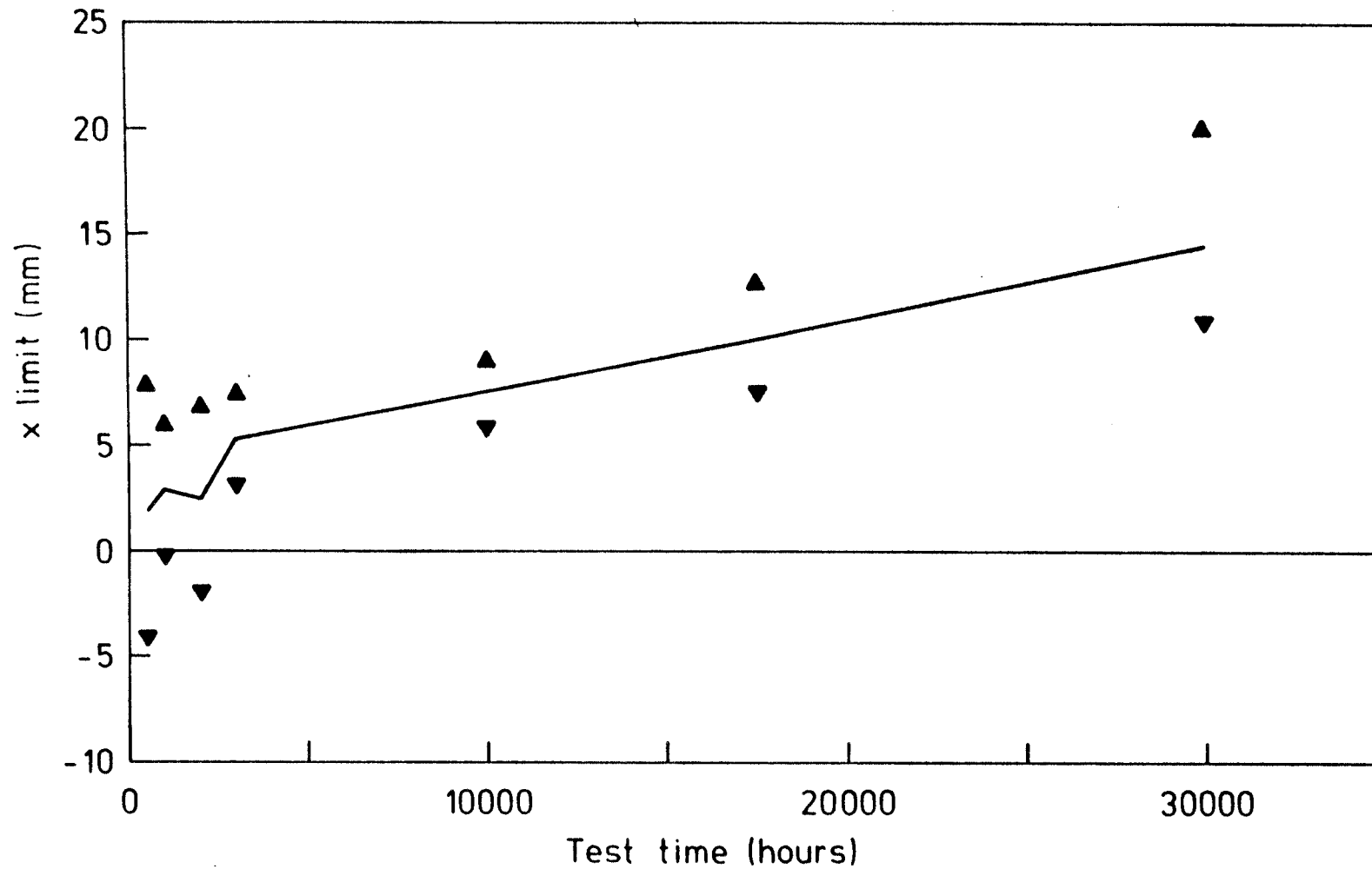
FIGURE 1. UPPER AND LOWER BOUND VALUES FOR THE MAXIMUM PROBABLE PIT DEPTH ESTIMATED FROM THE UNLIMITED DISTRIBUTION FUNCTION FOR THE UK – DOE / CEC PROGRAMME DATA
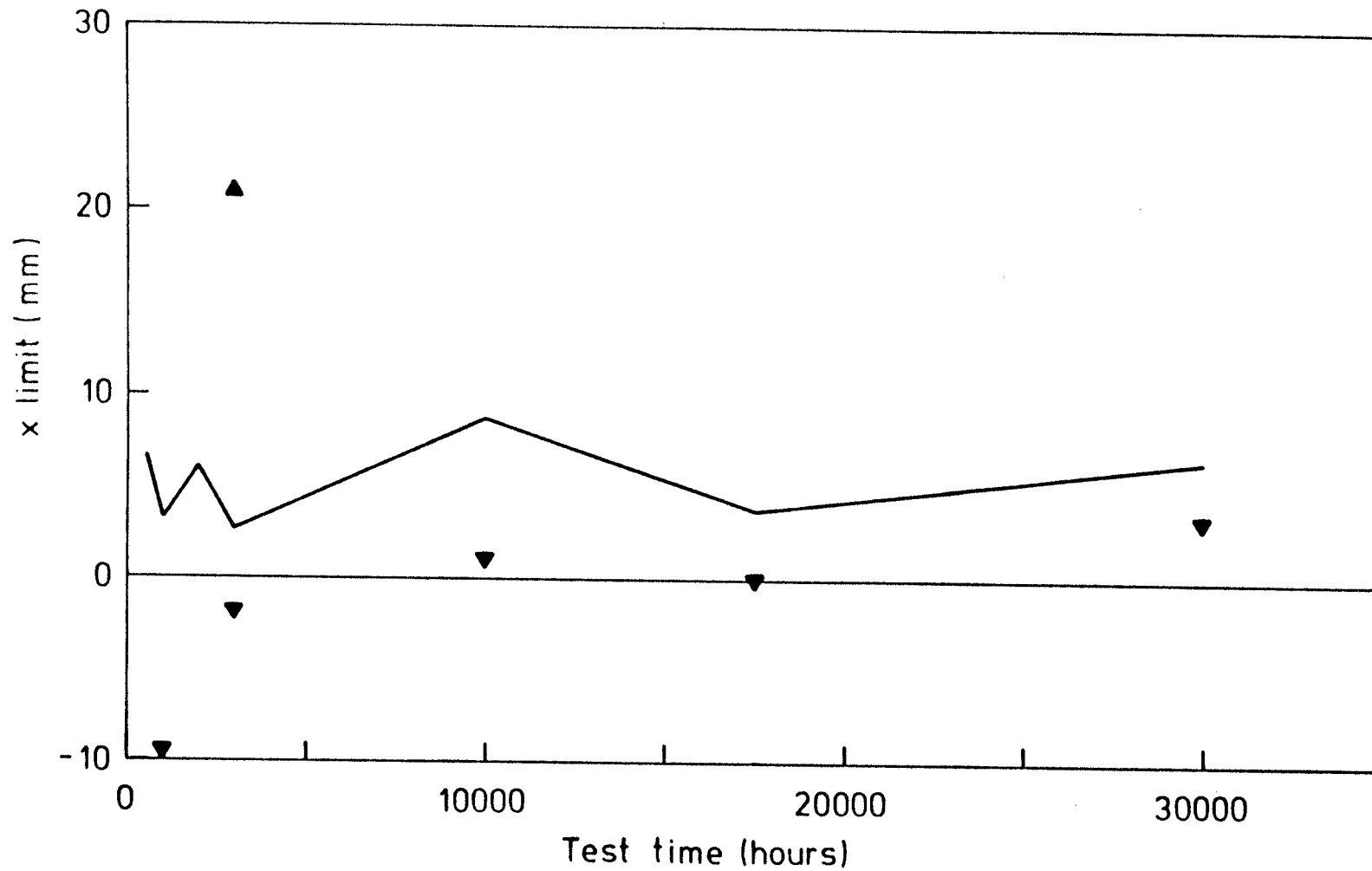
FIGURE 2 UPPER AND LOWER BOUNDS FOR THE LIMITING PIT DEPTH ESTIMATED FROM THE GENERALISED DISTRIBUTION FUNCTION FOR UK – DOE / CEC PROGRAMME DATA
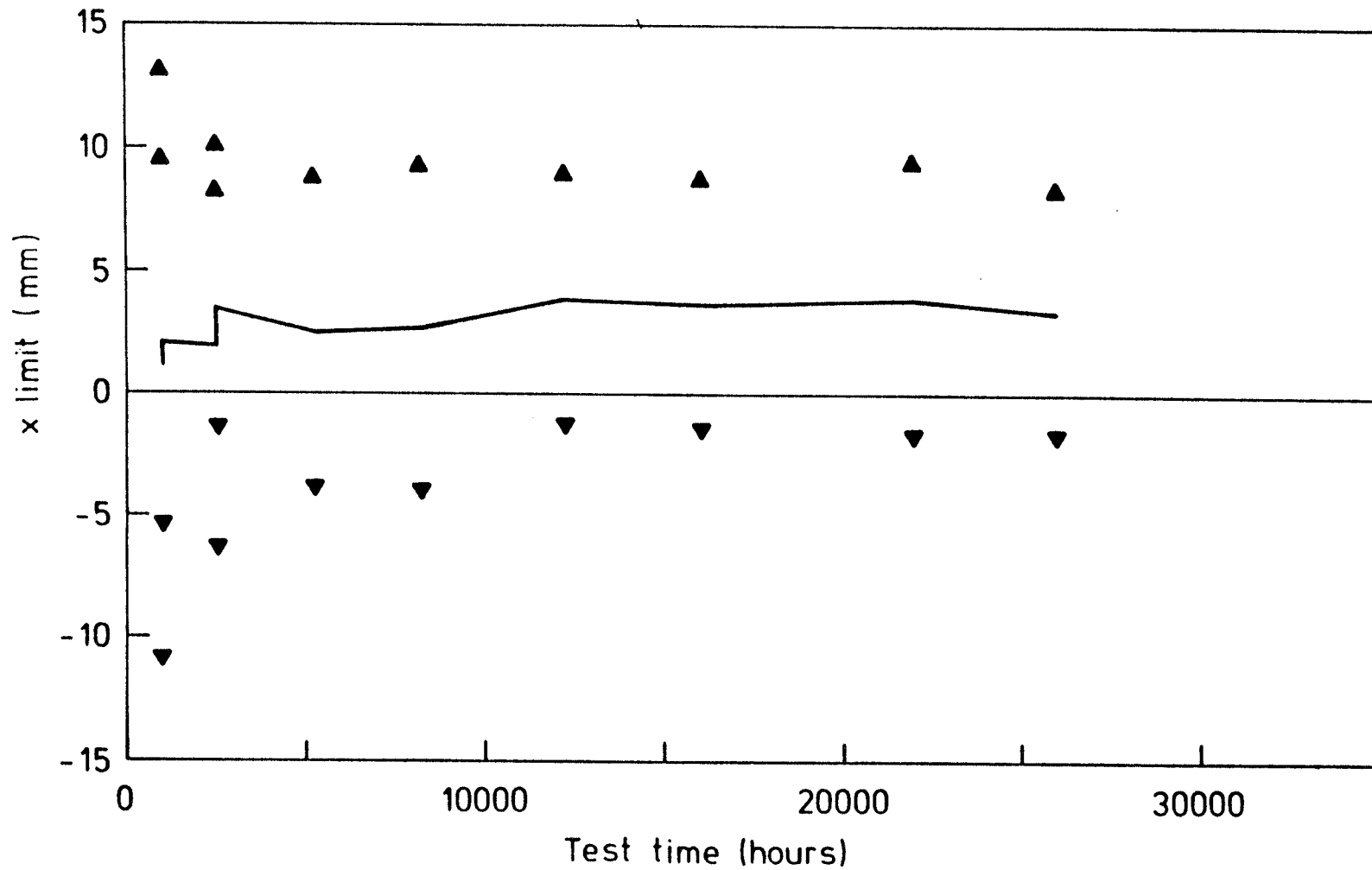
FIGURE 3. UPPER AND LOWER BOUND VALUES FOR THE MAXIMUM PROBABLE PIT DEPTH ESTIMATED FROM THE UNLIMITED DISTRIBUTION FUNCTION FITTED TO PIT GROWTH RESULTS FROM TESTS AT 90°C
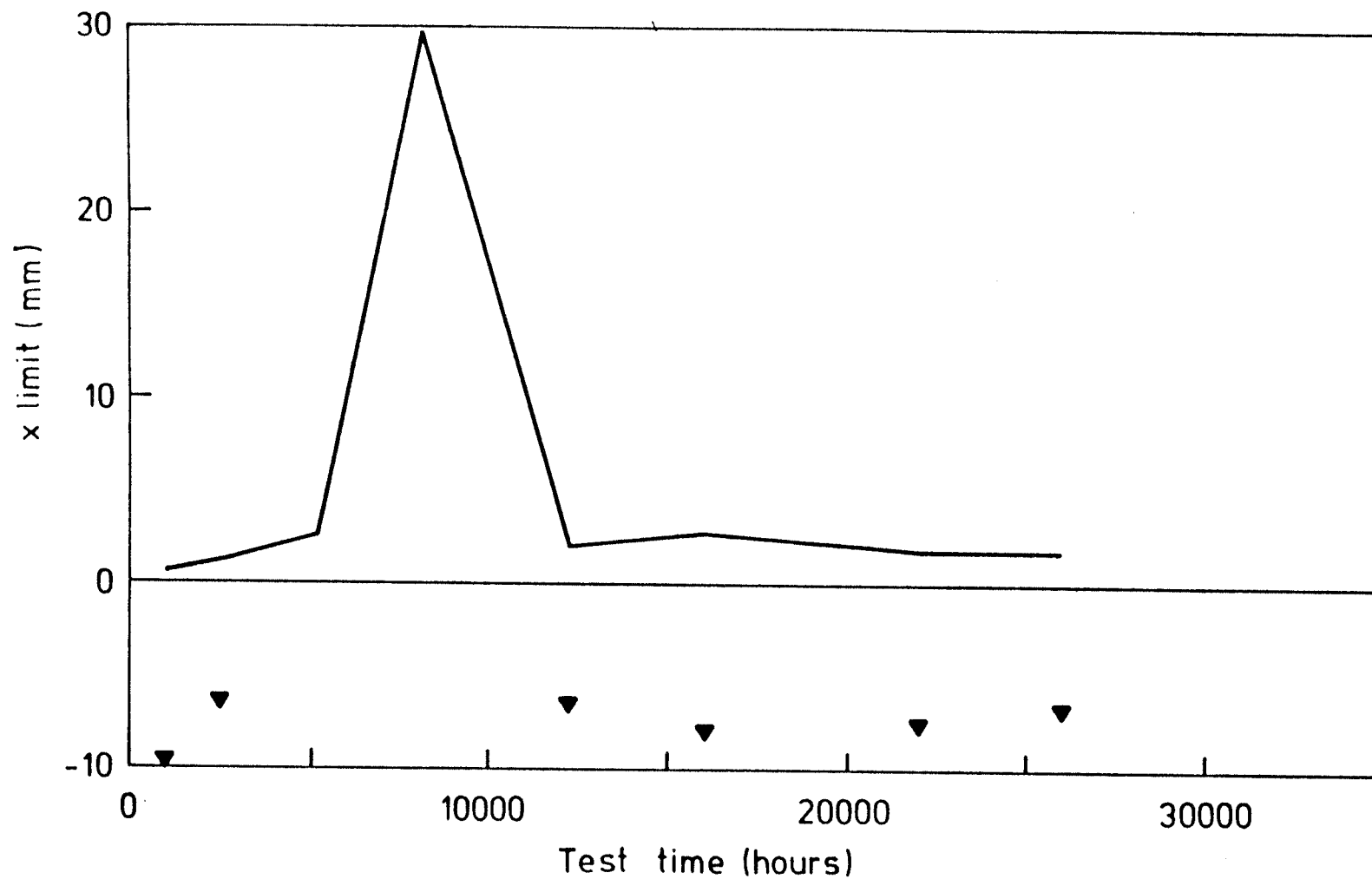
FIGURE 4. UPPER AND LOWER BOUNDS FOR THE LIMITING PIT DEPTH ESTIMATED FROM THE GENERALISED DISTRIBUTION FUNCTION FITTED TO PIT GROWTH DATA FROM TESTS AT 90°C
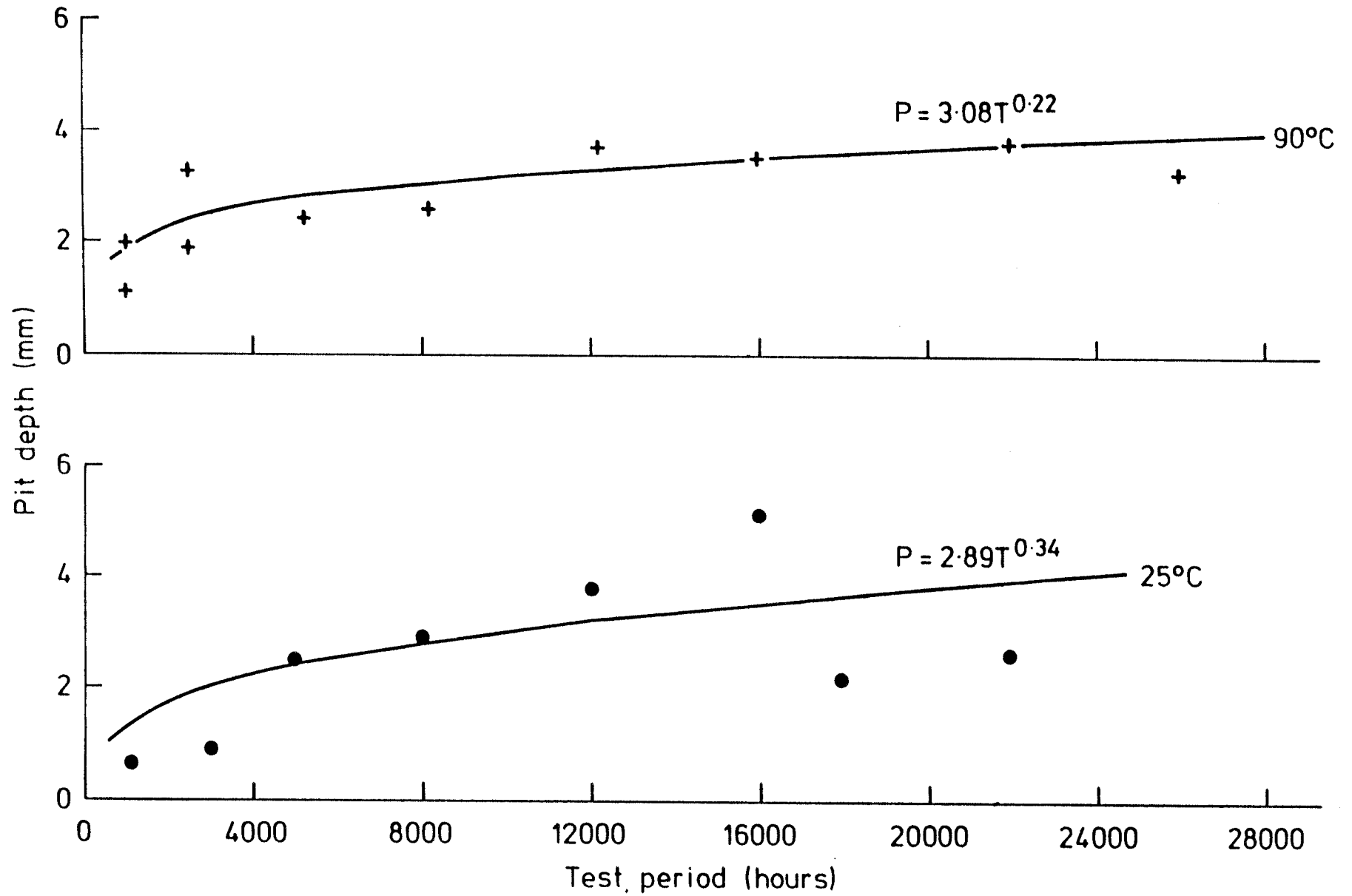
FIGURE 5 PIT DEPTH WITH 0·1 PROBABILITY OF BEING EXCEEDED ACCORDING TO TYPE I DISTRIBUTION. GALVANOSTATIC CONTROLLED TESTS AT 25° AND 90°C.
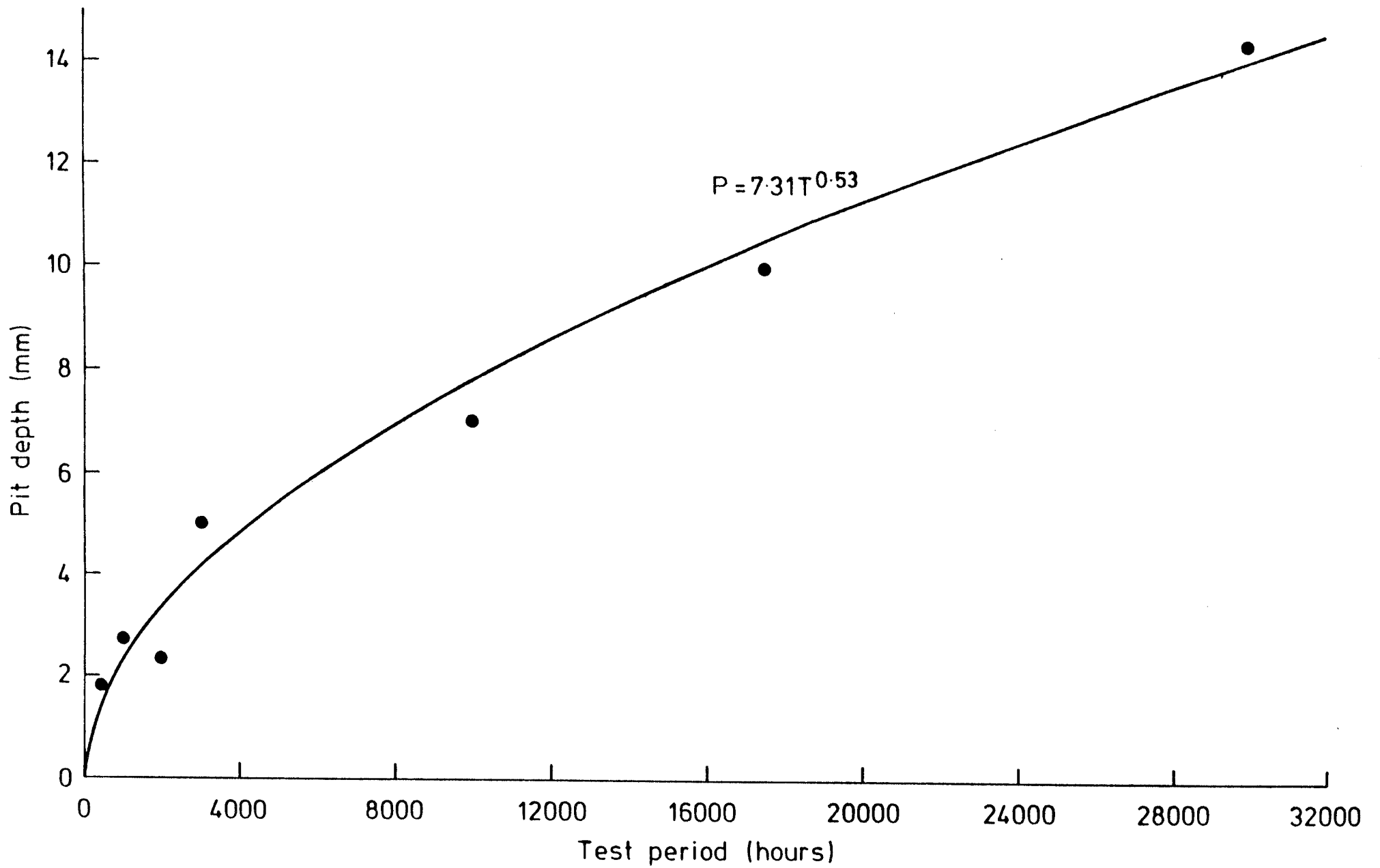
FIGURE 6 PIT DEPTH WITH 0·1 PROBABILITY OF BEING EXCEEDED ACCORDING TO TYPE I DISTRIBUTION. UK-DOE/CEC TESTS AT 90°C WITH POTENTIOSTATIC CONTROL.

20G 1002H

21G 2514H

20AG/0.1M,1000ppm /GC/90C/5232h

24G/0.1M,1000ppm/GC/90C/8208h

22AG/GC/90C/12234h

25AG/GC/90C/16048h

FIGURE 7 THE DEVELOPMENT OF LOCALISED CORROSION WITH EXPOSURE FOR THE TESTS AT 90C

W3/GC/90C/1025h

W4/GC/90C/3014h

W4/2-GC-90C-5018h

W3/2-GC/90C/7990h

W1/GC/90C/9970h

W2/GC/90C/15096h

FIGURE 8 THE DEVELOPMENT OF LOCALISED CORROSION
IN PLATES CONTAINING A PENETRATION
AUTOGENOUS ELECTRON BEAM WELD
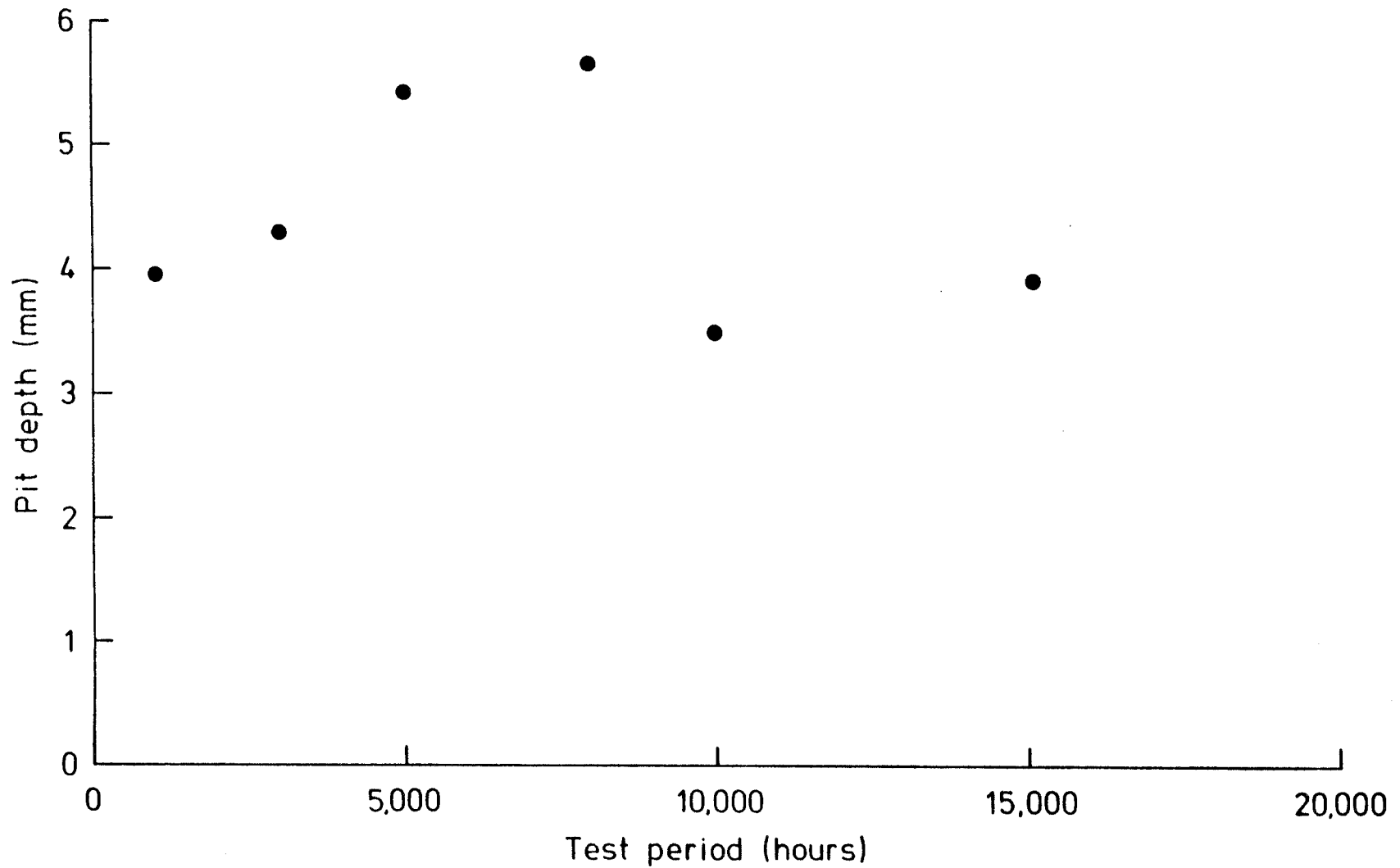
FIGURE 9 PIT DEPTH WITH 0·1 PROBABILITY OF BEING EXCEEDED, TYPE I DISTRIBUTION.
GALVANOSTATIC CONTROL ON WELDED PLATES AT 90°C.
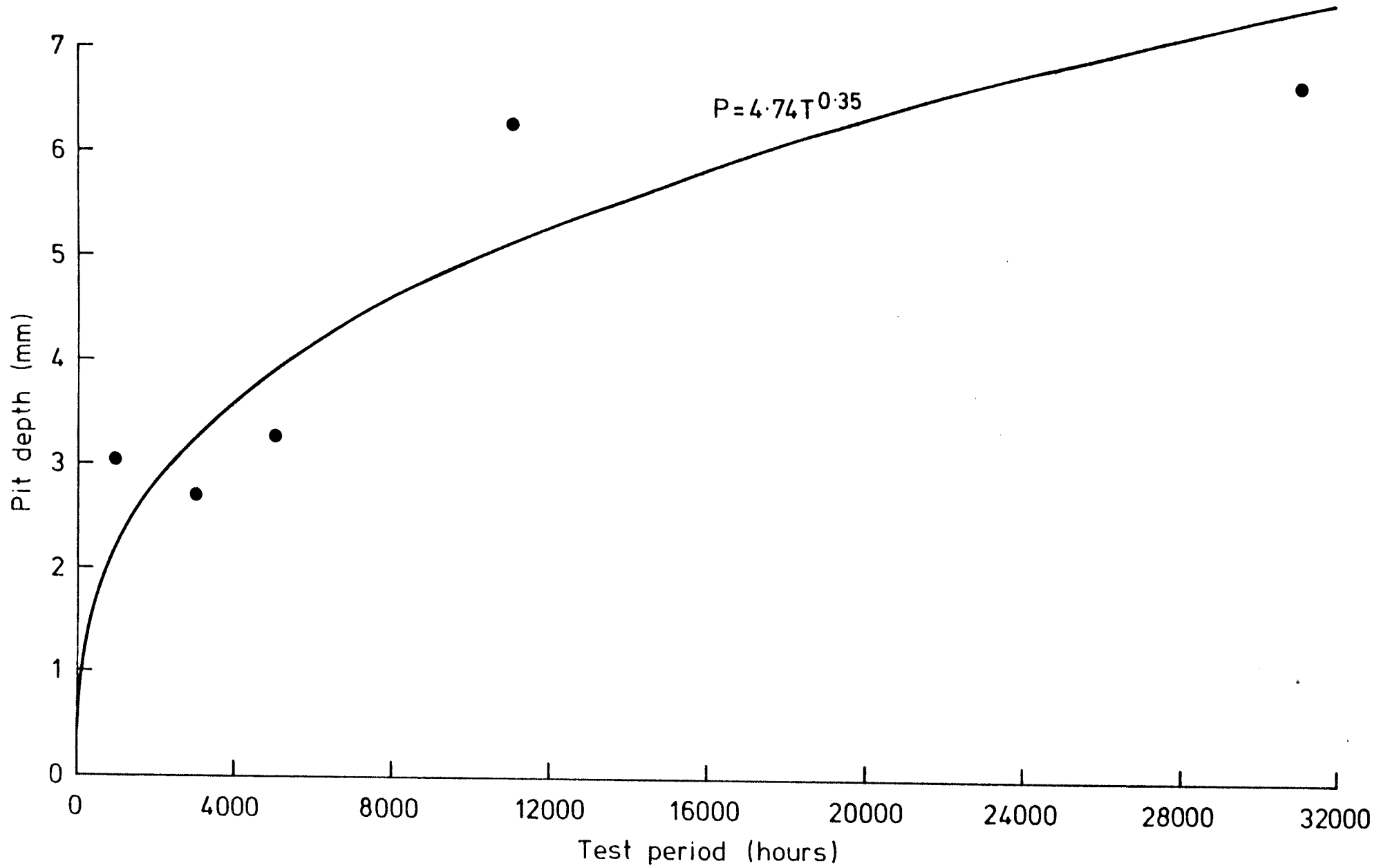
FIGURE 10 PIT DEPTH WITH 0·1 PROBABILITY OF BEING EXCEEDED, TYPE I DISTRIBUTION. OXYGENATED SOLUTION AT 50°C.
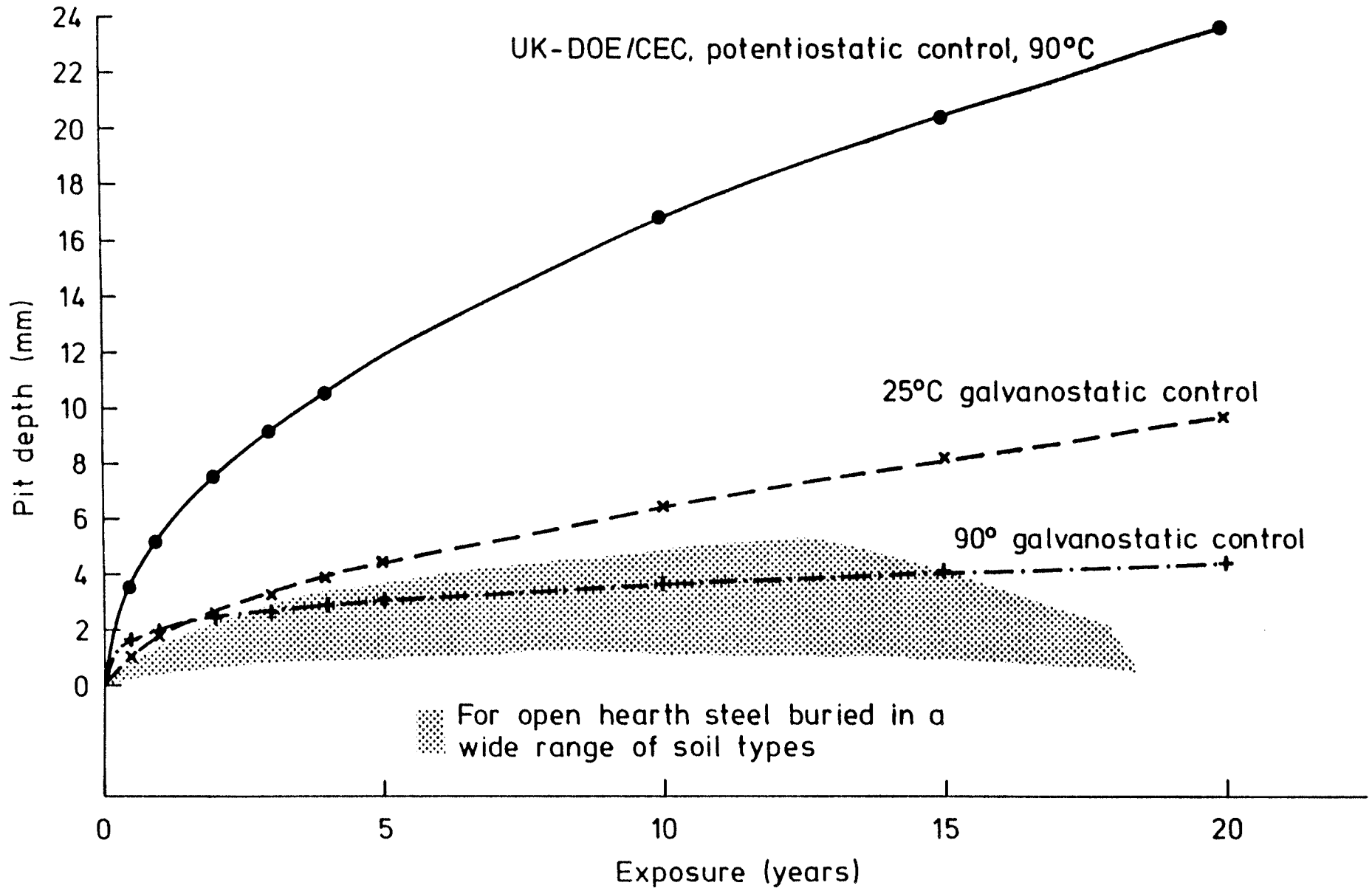
FIGURE 11 COMPARISON OF DEEPEST PITS FROM ROMANOFF (REF.7) WITH EXPERIMENTAL PLOTS EXTRAPOLATED TO SAME SURFACE AREA WITH 0·1 PROBABILITY OF BEING EXCEEDED

Pit radius (mm)
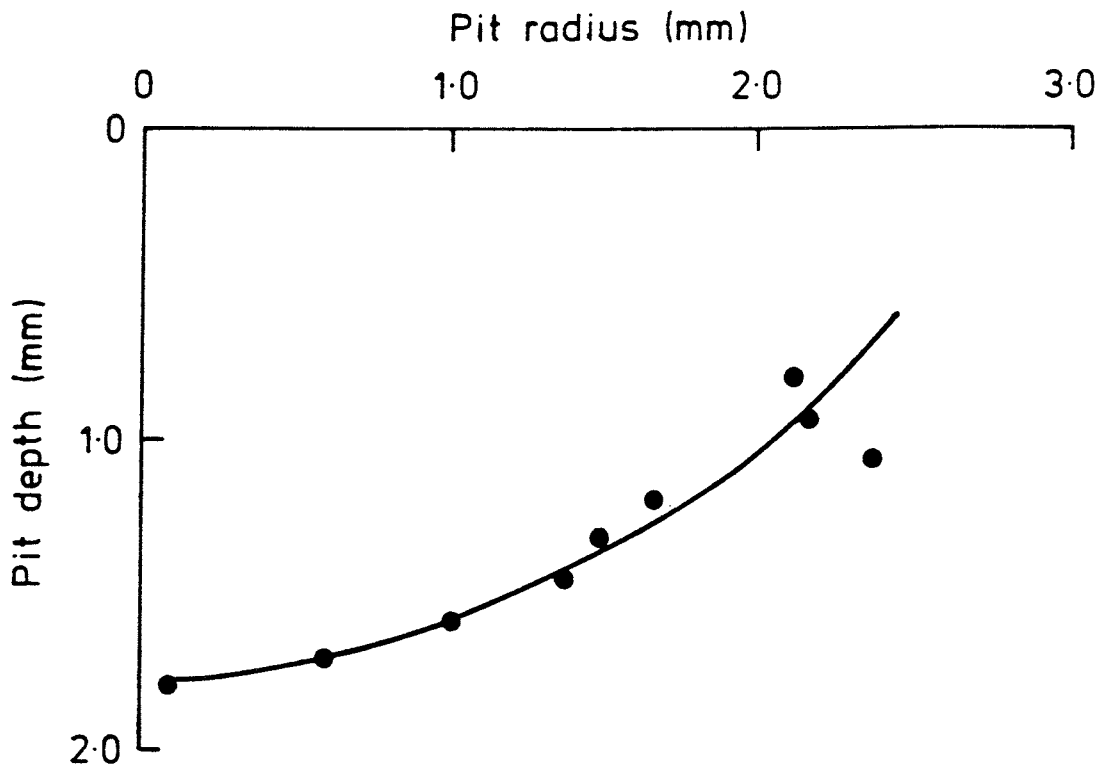
(a) 5,009 hours exposure at ambient temperature

Pit radius (mm)
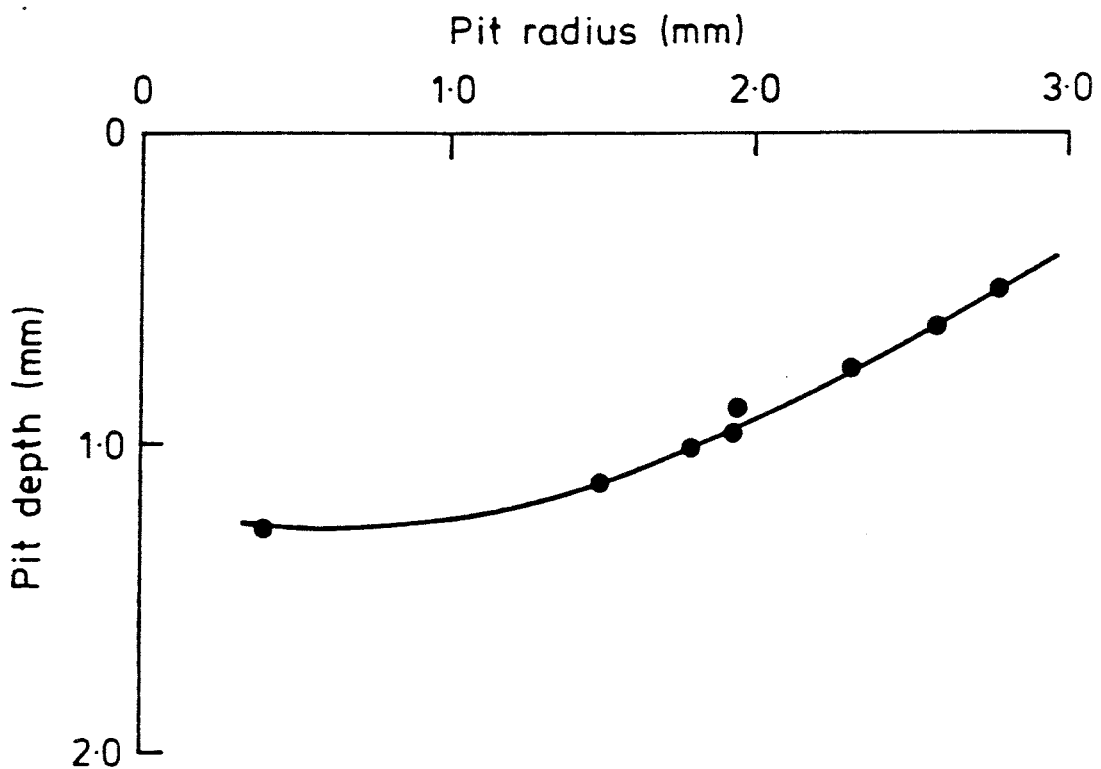
(b) 16,048 hours exposure at 90°C

FIGURE 12. PIT CROSS SECTIONS FROM TESTS IN 0·1M NaHCO$_3$ + 1000ppm Cl$^-$ SOLUTION. GALVANOSTATIC CONTROL (5μA cm^{-2})
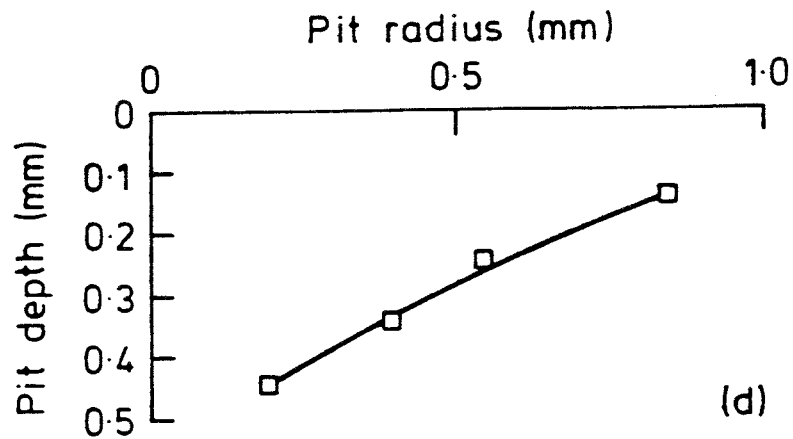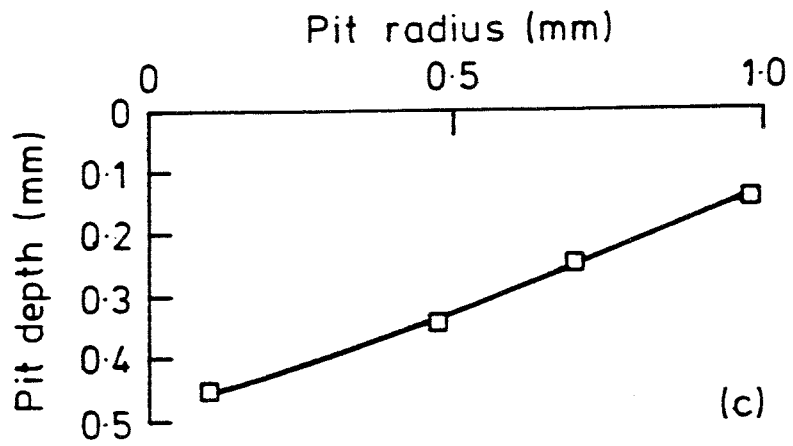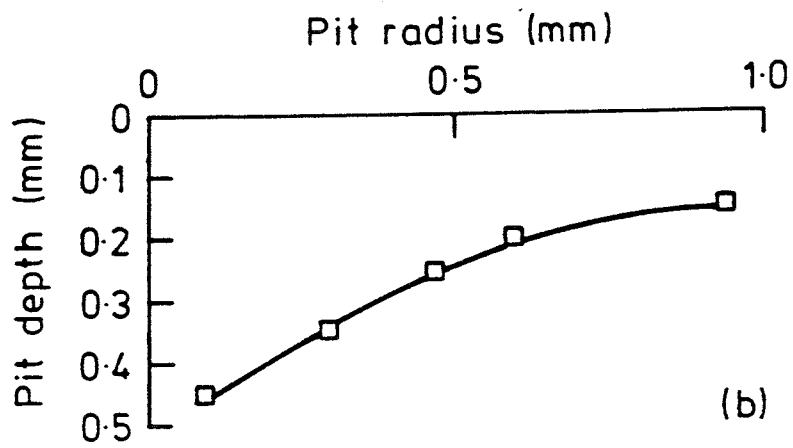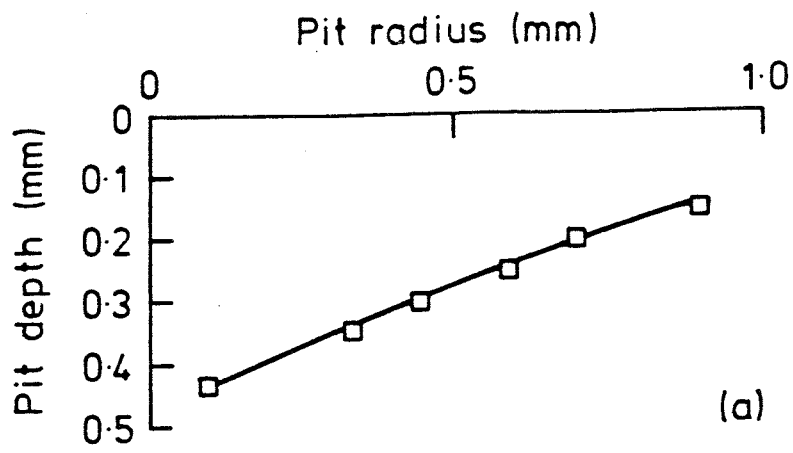
FIGURE 13 PIT CROSS SECTIONS FROM TESTS (REF 9) IN
0·1M NaHCO$_3$ + 1000ppm Cl$^-$ SOLUTION AT 90°C
UNDER POTENTIOSTATIC CONTROL (-200 mV/SCE)
1000 HOURS EXPOSURE
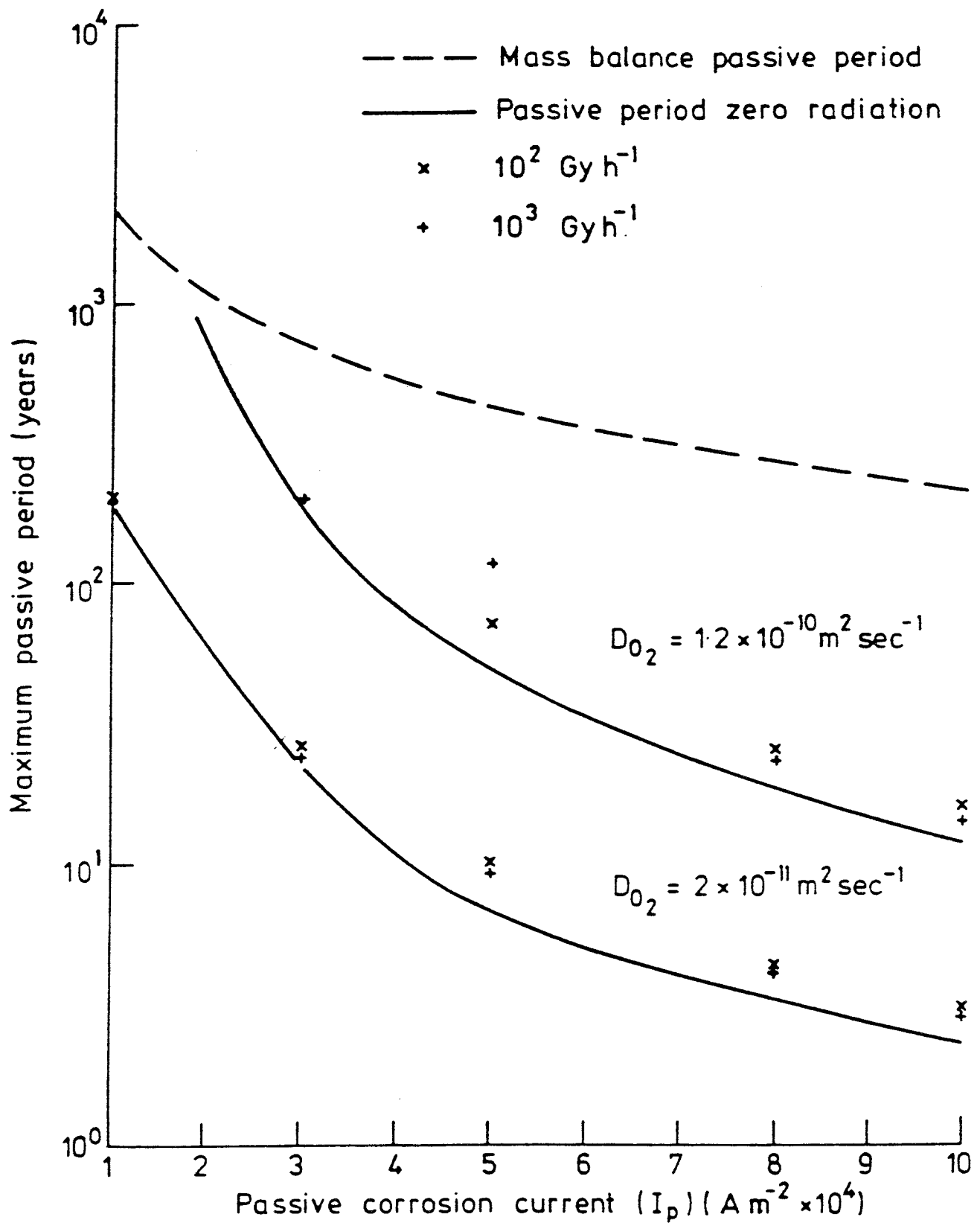
FIGURE 14 . INFLUENCE OF DIFFUSION RATE AND RADIATION DOSE RATE UPON THE MAXIMUM PASSIVE PERIOD OVER A RANGE OF PASSIVE CORROSION RATES

APPENDIX
Fitting Procedures for Corrosion Pit Data

CONTENTS

Contents

1 Fitting and Statistical Procedures

This appendix describes the fitting procedures and statistical methods which were used in fitting and analysing the experimental data. We begin with a brief summary of the method used for fitting nonlinear functions to data. This is followed by the description of the χ^2 fitting criterion adopted.

A non-linear fitting procedure has been used throughout, rather than adopting the strategy of first linearizing the data and then using conventional regression. The method used is Marquardt's, as described by Press *et al* (1986). This is a compromise between a steepest-descents method and Newton's method. In the steepest descent approach, at each point in the minimisation procedure a step is taken down the gradient of the surface, measured at the starting point. More mathematically, we are trying to minimize a function $F(\mathbf{x})$ of n variables, where

$$\mathbf{x} = (x_1, ... x_n)^T.$$

Write the vector of partial derivatives as

$$\mathbf{F'} = (\partial F/\partial x_1, ..., \partial F/\partial x_n),$$

and at step i make a downhill step in the direction of the gradient of the function $\mathbf{F'}(\mathbf{x}^i)$,

$$\mathbf{x}^{i+1} = \mathbf{x}^i - \delta\mathbf{F'}(\mathbf{x}^i)$$

where δ is a small parameter. In most cases, however, the local gradient does not point towards the true minimum $\mathbf{x}_0$, and the path towards the minimum is very indirect as the direction of the steepest descent path swings to and fro. To steer the minimisation more effectively one may adopt the Newton-Raphson method, which uses the matrix of second derivatives

$$\mathbf{F''} = \begin{pmatrix} \partial^2 F/\partial x_1 \partial x_1 & \cdots & \partial^2 F/\partial x_1 \partial x_n \\ \vdots & \ddots & \vdots \\ \partial^2 F/\partial x_n \partial x_1 & \cdots & \partial^2 F/\partial x_n \partial x_n \end{pmatrix}$$

We suppose that, close to the minimum, the function F may be written

$$F(\mathbf{x}) \approx F_0 + \mathbf{F'} \cdot (\mathbf{x} - \mathbf{x}_0) + \frac{1}{2}(\mathbf{x} - \mathbf{x}_0) \cdot \mathbf{F''} \cdot (\mathbf{x} - \mathbf{x}_0).$$

Then it is straightforward to move from the current estimate of x, x^i say, to the next estimate x^{i+1}. At the minimum the gradient of F is zero, that is

$$F''(x_0) \cdot x_0 = -F'(x_0),$$

whereas at the current point

$$F'(x^i) = F'(x_0) + F''(x_0) \cdot x^i,$$

so that subtracting these two equations and multiplying by $F''(x_0)^{-1}$ gives

$$x^{i+1} = x^i - F''(x_0)^{-1} \cdot F'(x^i).$$

Of course, one does not know the value of F'' at the minimum, x_0. Indeed, in general one does not know the second derivative matrix F'' exactly at any point, but builds up an approximation to it as the minimisation proceeds. We denote this approximation at step i by $F''^{(i)}$. There are two problems. First, one may be sufficiently far from the minimum that the expansion to second order is not a good approximation, and the use of the second derivative matrix may send one off in the wrong direction. Second, the current approximation to the second derivative matrix may not be positive definite, so that by using it one may actually increase the value of the objective function rather than reducing it.

A reliable method has been devised (by Marquardt, following earlier work by Levenberg) which switches steadily from steepest descents to Newton's method as the minimum is approached. The method relies on the observation that for any matrix A then if P is positive definite so is $A + \lambda P$ for sufficiently large λ. Marquardt suggested that P should be taken as a diagonal matrix, with elements the absolute values of the diagonal elements in the approximate $F''^{(i)}$ (or unity if the diagonal element is zero). Then if the formula for each step is written as

$$x^{i+1} = x^i - [F''^{(i)} + \lambda^{(i)} P^{(i)}]^{-1} \cdot F'(x^i)$$

we see that as $\lambda^{(i)}$ tends to zero we recover Newton's method, but as $\lambda^{(i)}$ tends to infinity we take very short steps in the steepest descent direction.

For the implementation of Marquardt's method we need to know the derivatives of the various fitting functions with respect to their parameters. We have computed these analytically, rather than by numerical differentiation.

2 Fitting procedure

We have used a χ^2 fitting criterion throughout the analysis. Thus, given a set of observations y_i which we believe to be described by a function of the independent variable t by a function F with parameters $\mathbf{x}$

$$y_i = F(\mathbf{x}|t_i)$$

we seek to minimise

$$\chi^2 = \sum_i [y_i - F(\mathbf{x}|t_i)]^2.$$

In the case of a probability distribution, where the observations y_i of the random variable η are believed to come from a probability density function $p(\mathbf{x}|\eta)$ with cumulative probability $F(\mathbf{x}|\eta)$, we proceed as follows. The cumulative probability F is estimated by counting the number of pits n_i in the specimen whose depths are greater than y_i and the total number of pits in the specimen N, and estimating

$$F_i = \frac{n_i}{N+1}.$$

Then the fitting procedure is to minimise

$$\chi^2 = \sum_i [F_i - F(\mathbf{x}|y_i)]^2.$$

Note that this differs slightly from the conventional method of fitting probability density functions, in which the range of observations is binned into disjoint intervals j being $[y_j^\vee, y_j^\wedge]$, the expected number of observations in each range computed,

$$E_j(\mathbf{x}) = N \int_{y_j^\vee}^{y_j^\wedge} p(\mathbf{x}|y)y,$$

and $\mathbf{x}$ determined so as to minimise

$$\chi^2 = \sum_j [N_j - E_j(\mathbf{x})]^2/E_j(\mathbf{x}),$$

where N_j is the number of observations in bin j, or, more commonly,

$$\chi^2 = \sum_j [N_j - E_j(\mathbf{x})]^2 / N_j.$$

This χ^2 method is, in common with the maximum likelihood method, consistent and asymptotically efficient (that is, in the limit when the N_j tend to infinity). Neither method, however, is very reliable for small amounts of data (the present situation). The maximum likelihood estimator is neither unbiased nor efficient for small samples. The χ^2 procedure is not accurate if there are fewer than about 5 obervations in each interval ($N_j > 5$): to maintain adequate resolution along the depth axis we frequently have only one observation in an interval.

We have used the χ^2 method throughout the present work. We have made some comparisons between the χ^2 method and the maximum likelihood method for the unlimited distribution (Type I) and find the results of the two methods to be very similar.

3   Nonlinear versus linearized fitting

There are two reasons for selecting a nonlinear fitting procedure. The first is that for the Type III and generalized extreme value distributions no simple linearizing transformation exists, so that a nonlinear procedure *must* be used. The other reason is more subtle, and is demonstrated in figures A1 and A2. Suppose we try to fit the data

t	y
1	1
3	2
9	3

to the function

$$y = At^b$$

by varying A and b. The traditional method of treating this problem was to transform it to the linear form

$$\bar{y} = \ln y = \ln A + bt$$

and to use linear regression. This has the disadvantage that the distribution of errors in the transformed variable $\bar{y}$ is not the same as that in the original variable y, and is in fact likely to be biased, so that whereas the errors in y may have zero mean those in $\bar{y}$ may not.

When we perform the fitting the result is that

$$y = \begin{cases} 1.116844t^{0.499969}, & \text{using linearized fit;} \\ 1.123989t^{0.453614}, & \text{using nonlinear fit.} \end{cases}$$

The resulting functions are significantly different, as shown in Figure A1 (plotted in linear form) and A2 (logarithmically). The important point is that if the errors in measuring the dependent variables are believed to be randomly distributed with standard deviation independent of y and zero mean, the nonlinear fitting procedure is the appropriate one.

4 Confidence Limits

As described above, Marquardt's method builds up an approximation to the Hessian matrix F''. In the χ^2 method, then, on completion of the minimisation one has an estimate of F'' which is the second derivative of χ^2 with respect to the parameters x. The covariance matrix of the parameters x is the inverse matrix F''^{-1}. To assess our confidence in the fitted values of x, we need to make the following assumptions:

1. the measurement errors are distributed normally;

2. the fit is good enough for the fitted parameters x to be contained in a region in which a linear transformation could be used (which does not imply that a linear procedure must be used for the fitting).

If these hold, then χ^2 is distributed as a chi-square distribution with $N - n$ degrees of freedom, where N is the number of observations and n is the number of fitted parameters (the dimensionality of x). The change in χ^2 which arises from a change δx in the parameter vector x is then

$$\Delta\chi^2 = \delta x \cdot F'' \cdot \delta x.$$

Note that this corresponds to an elliptical region in x-space if $n = 2$, an ellipsoidal region with $n = 3$. The ellipse or ellipsoid may be most readily described in terms of its principal axes, formed from the eigenvectors of the matrix F'', and the corresponding eigenvectors. We find the n eigenvectors from

$$F'' v_i = \lambda_i v_i$$

and then

$$\Delta\chi^2 = \sum_{i=1}^{n} \lambda_i (\delta x \cdot v_i)^2.$$

The spread of the parameters x may then be estimated from the extremes of the ellipsoid in the direction corresponding to the maximum eigenvalue. The magnitude of the eigenvalue measures the spread of values, the direction of the eigenvector allows for the correlations among the parameters. We take the confidence limits, then, as

$$x_{\pm} = x_0 \pm \frac{\sqrt{\Delta\chi^2}}{\sqrt{\lambda_1}} v_1,$$

where x_0 corresponds to the minimum value of χ^2 and we take $\Delta\chi^2$ to correspond to the 90 percent confidence limit, taken from the table below.

$\Delta\chi^2$ for various confidence levels p and degrees of freedom ν		
p	ν	
68.3%	1.00	2.30	3.53
90%	2.71	4.61	6.25
95.4%	4.00	6.17	8.02
99%	6.63	9.21	11.3
99.73%	9.00	11.8	14.2
99.99%	15.1	18.4	21.1

5   Comments on the Fitting

The values reported in the tables show the values of χ^2 achieved with the best fit to the cumulative distribution functions. On the basis of these the generalised distribution function is uniformly better than the unlimited (Type I) function, and better than the limited (Type II) function except where it is identical with it. When one considers the *significance*, that is, considers the probability distribution function for χ^2 with $N - 2$ degrees of freedom (Type I) or $N - 3$ (Type III or generalised) the differences are marginal. Figure A3 shows the significance levels of the fits to the various sets of data: they are plotted as a function of time merely as a way of spreading out the results, but it is interesting that there is a trend to move from the unlimited (Type I) fits being more significant at short times and the generalized being marginally favoured at longer times. Overall, there is little evidence from this figure of the generalized distribution being favoured.

The main problem with the generalized distribution is that the parameters are strongly correlated and that there is quite a large region of parameter space in which the value of χ^2 only varies slowly. This is illustrated in Figure A4, which shows how the overall fit using the generalized distribution varies if the parameter β is held fixed and the fit performed only with α and d. The point that emerges is the flatness of the distribution for values of β between -0.1 and +0.05. This confirms that there is overall no clear evidence for a value of β different from zero, that is, that the unlimited (Type I) distribution is as good at describing the data as the generalized.

6   Time Development

Following the determination of the parameters of the extreme value distributions, we have computed a limiting depth $\hat{y}_i$ at each experimental duration t_i such that the probability of such a pit depth being exceeded within that time is less than 0.1. These limiting pit depths have then been fitted, using the nonlinear procedure, by

$$\hat{y} = At^b.$$

In each case the limiting depths with the optimal parameters x_0 and the depths obtained using the confidence-limit values of the extreme value distribution parameters $x_\pm$ have been obtained. The results are shown in Figure A5 for the UK-DoE/CEC data, in Figure A6 for the present data at ambient temperature, and in Figure A7 for the present data at 90 Centigrade. In each case the square symbols represent the limiting depths from the optimal parameters, the solid line the fitted expression $\hat{y} = At^b$, and the triangles and dashed lines are the corresponding results for the upper and lower confidence limits. The fitting parameters are given below, for depths in mm and time in years.

Experiment	Parameters	A	b
UK DoE/CEC	Optimal	7.30620	0.52764
	Lower limit	4.08561	0.82126
	Upper limit	10.89641	0.40628
25 Degree	Optimal	2.89374	0.34331
	Lower limit	-2.95989	-0.77662
	Upper limit	9.66062	-0.19465
90 Degree	Optimal	3.07867	0.21903
	Lower limit	-2.43919	-0.54066
	Upper limit	9.21793	-0.07011

It should be noted that the spread of values arising from the uncertainties in the parameters of the extreme value distributions are greater than those in the fitting of the limiting depths to At^b. The negative exponents found in the fitting of the confidence limit data is an expression of the greater accuracy of the extreme value distribution parameters, requiring the upper and lower limits to converge on the line of the optimal results, at longer times.

References

W.H. Press, B.P. Flannery, S.A. Teukoisky and W.T. Vetterling (1986) *Numerical Recipes*, Cambridge University Press.

FIGURE A1 COMPARISON OF FITTING PROCEDURES
Linearised versus Nonlinear
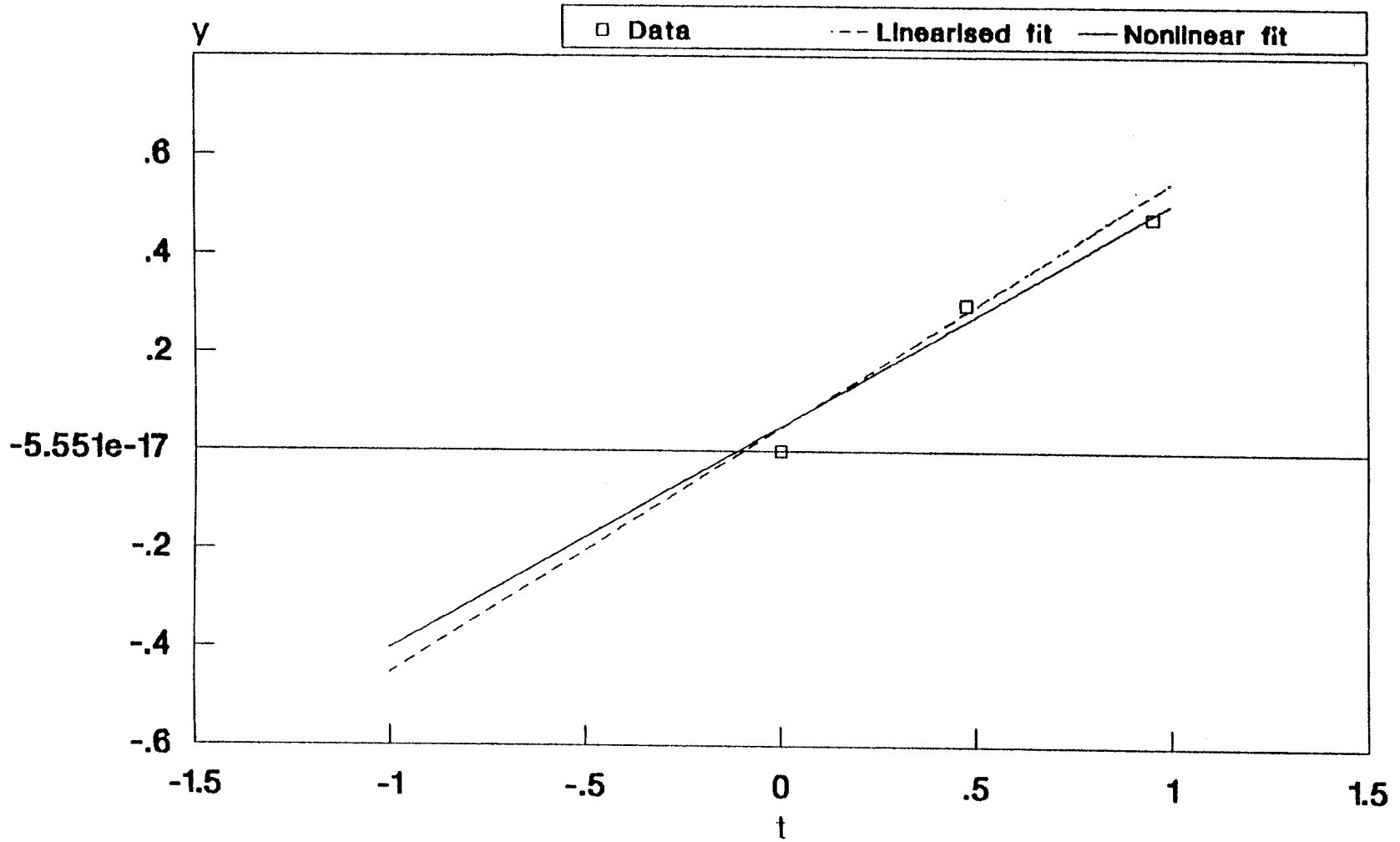
$y = a\ t\hat{\ }b$

FIGURE A2 COMPARISON OF FITTING PROCEDURES
Linearised versus Nonlinear

$y = a \ t^\wedge b$

FIGURE A3 Extreme Value Statistics (ex rpt)
All data
Significance levels
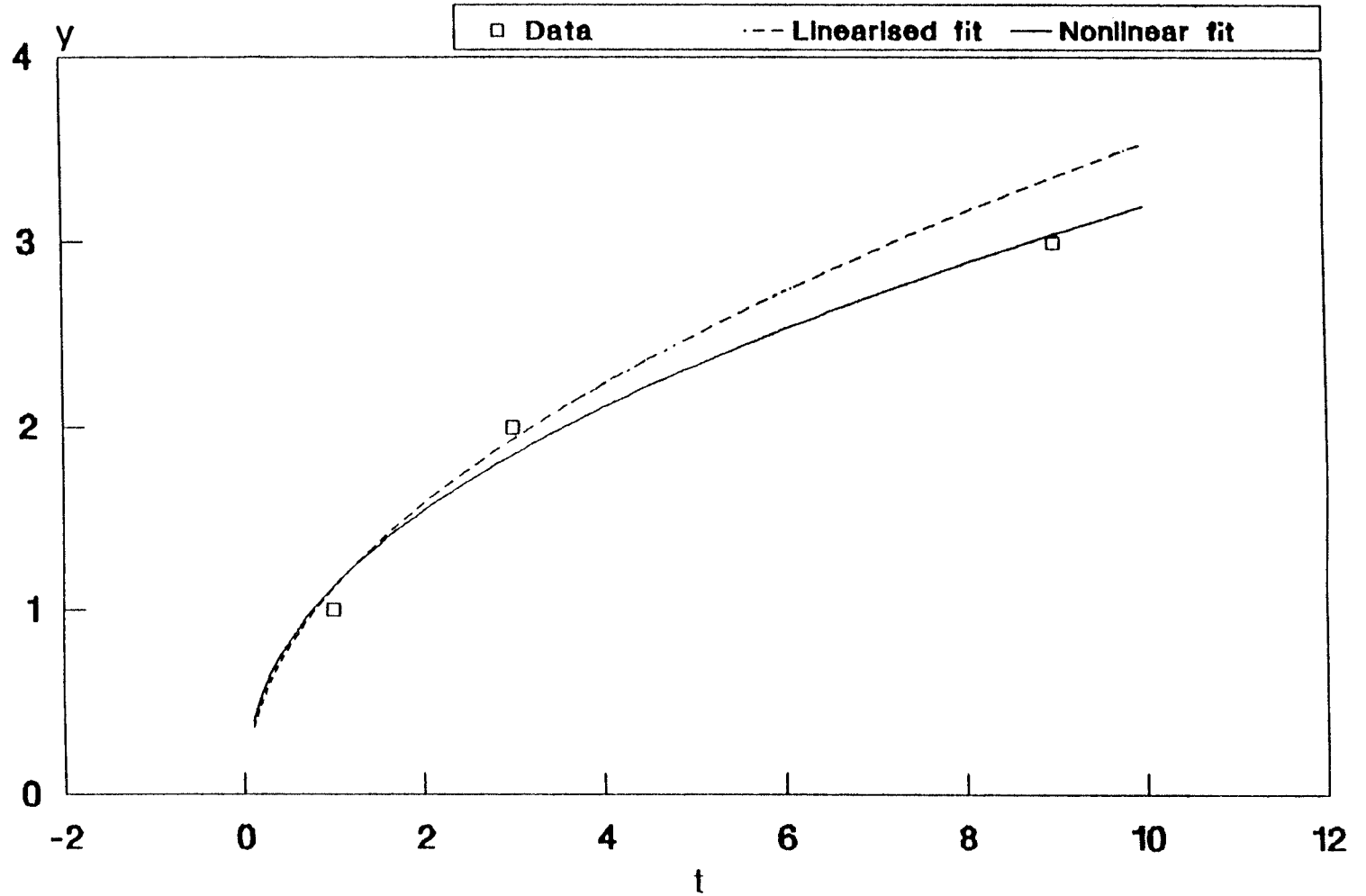
GEV Distribution
FIGURE A4 Mean chi-squared as function of β
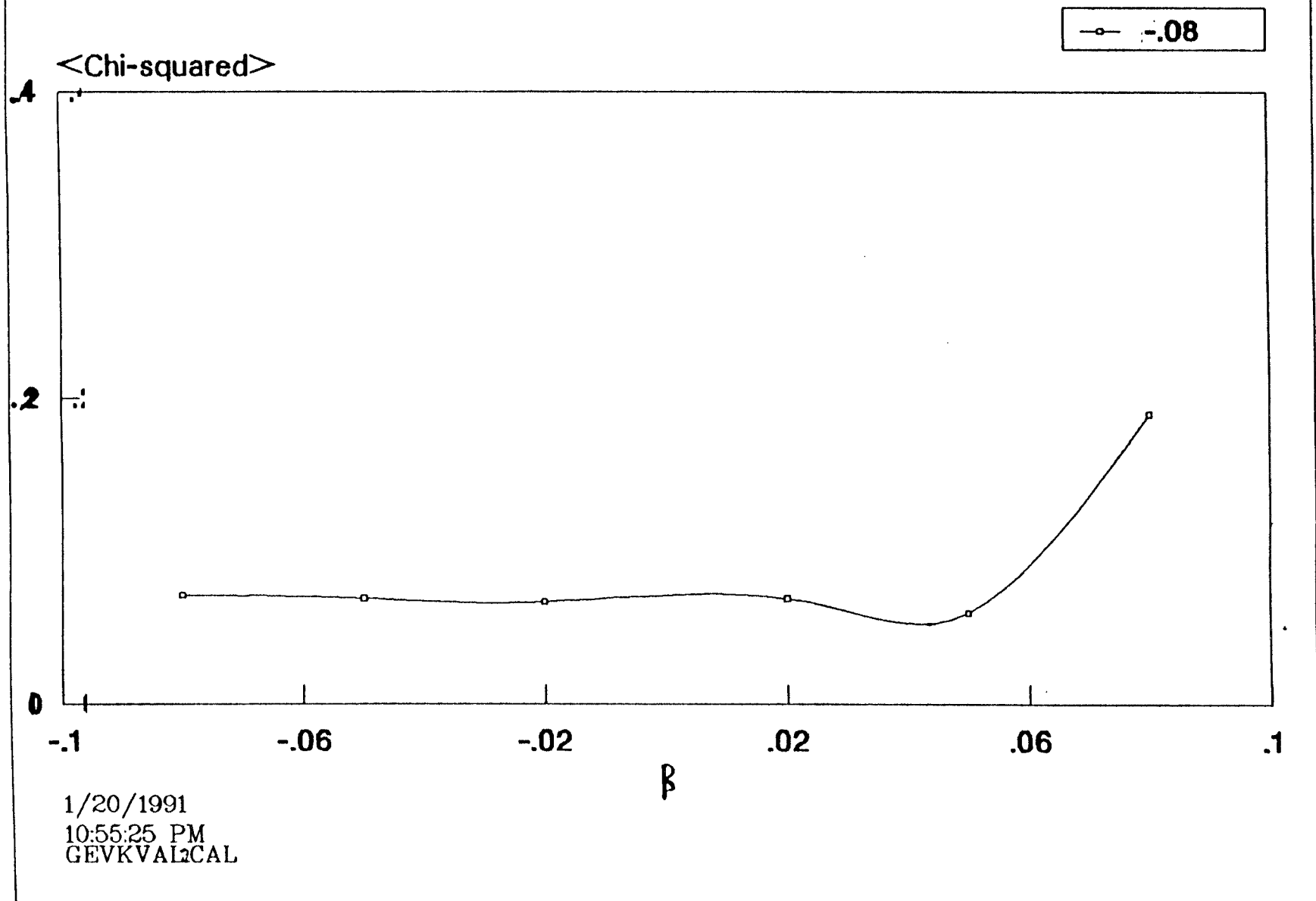
FIGURE A5 Trends of Limiting Depths
Unlimited Distribution
UK-DOE/CEC DATA
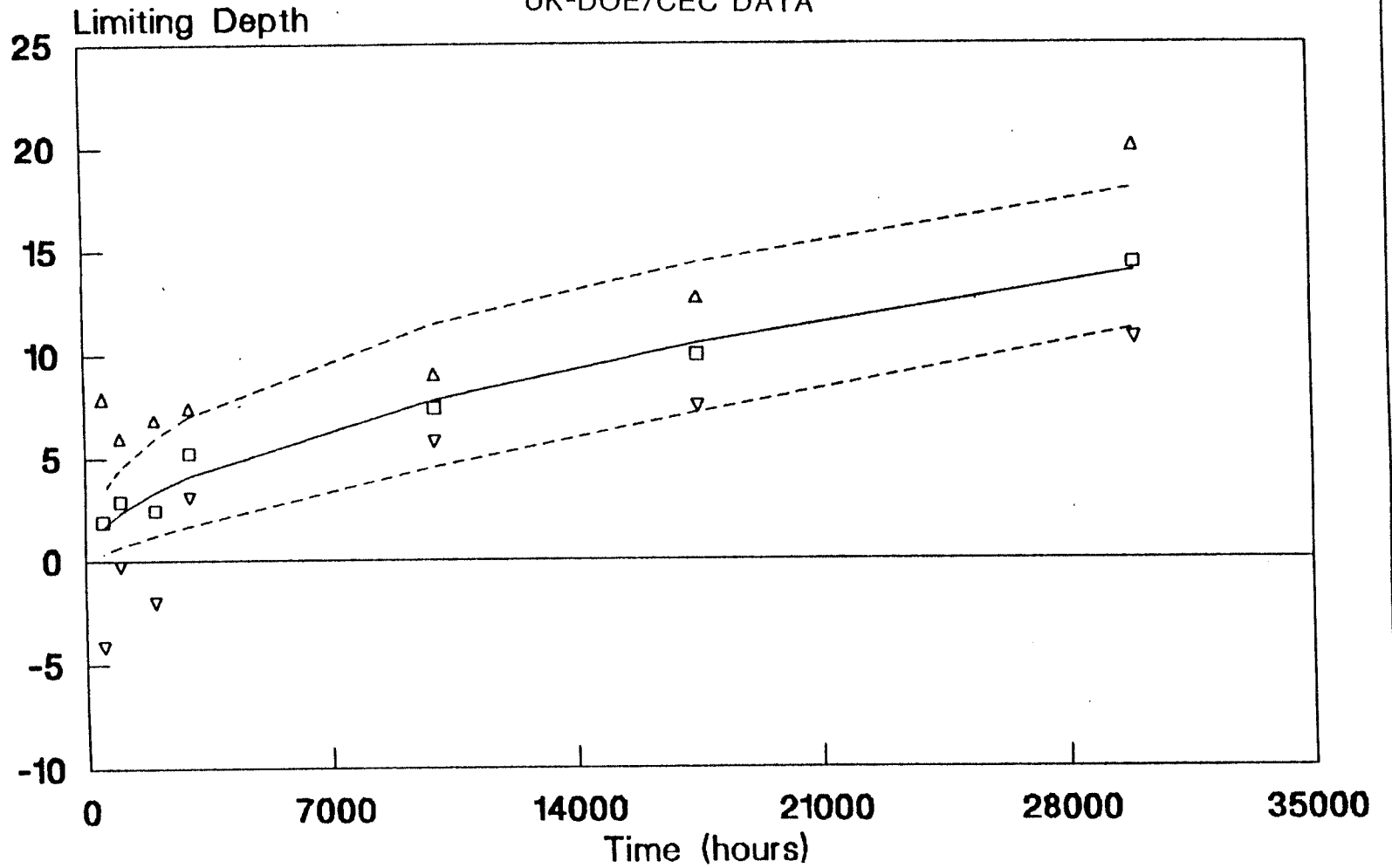
FIGURE A6 Trends of Limiting Depths
Unlimited Distribution
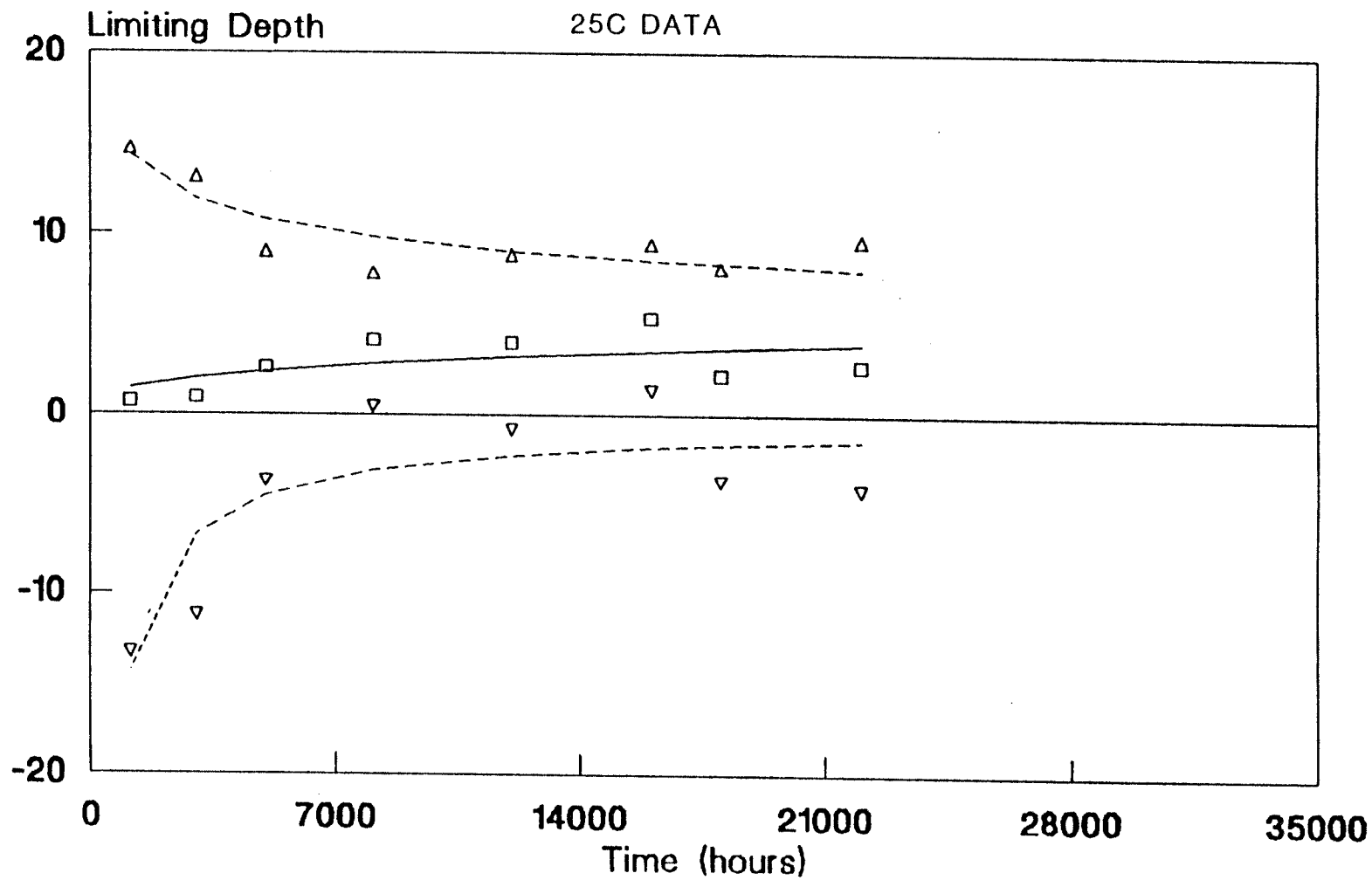
FIGURE A7 Trends of Limiting Depths
Unlimited Distribution
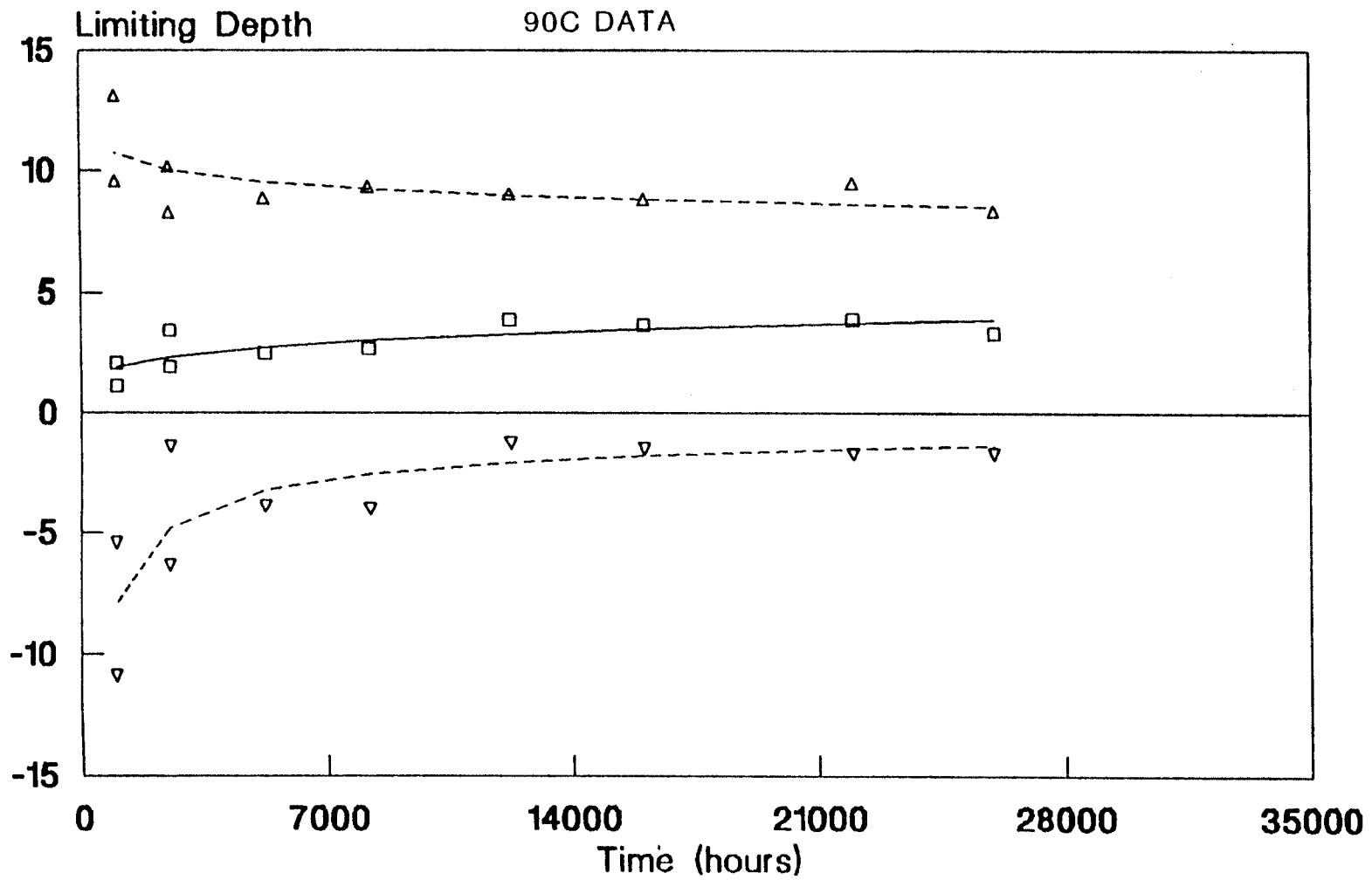
List of SKB reports

Annual Reports

1977-78
TR 121
KBS Technical Reports 1 – 120
Summaries
Stockholm, May 1979

1979
TR 79-28
The KBS Annual Report 1979
KBS Technical Reports 79-01 – 79-27
Summaries
Stockholm, March 1980

1980
TR 80-26
The KBS Annual Report 1980
KBS Technical Reports 80-01 – 80-25
Summaries
Stockholm, March 1981

1981
TR 81-17
The KBS Annual Report 1981
KBS Technical Reports 81-01 – 81-16
Summaries
Stockholm, April 1982

1982
TR 82-28
The KBS Annual Report 1982
KBS Technical Reports 82-01 – 82-27
Summaries
Stockholm, July 1983

1983
TR 83-77
The KBS Annual Report 1983
KBS Technical Reports 83-01 – 83-76
Summaries
Stockholm, June 1984

1984
TR 85-01
Annual Research and Development Report 1984
Including Summaries of Technical Reports Issued
during 1984. (Technical Reports 84-01 – 84-19)
Stockholm, June 1985

1985
TR 85-20
Annual Research and Development Report 1985
Including Summaries of Technical Reports Issued
during 1985. (Technical Reports 85-01 – 85-19)
Stockholm, May 1986

1986
TR 86-31
SKB Annual Report 1986
Including Summaries of Technical Reports Issued
during 1986
Stockholm, May 1987

1987
TR 87-33
SKB Annual Report 1987
Including Summaries of Technical Reports Issued
during 1987
Stockholm, May 1988

1988
TR 88-32
SKB Annual Report 1988
Including Summaries of Technical Reports Issued
during 1988
Stockholm, May 1989

1989
TR 89-40
SKB Annual Report 1989
Including Summaries of Technical Reports Issued
during 1989
Stockholm, May 1990

1990
TR 90-46
SKB Annual Report 1990
Including Summaries of Technical Reports Issued
during 1990
Stockholm, May 1991

Technical Reports
List of SKB Technical Reports 1991

TR 91-01
Description of geological data in SKB's database GEOTAB
Version 2
Stefan Sehlstedt, Tomas Stark
SGAB, Luleå
January 1991

TR 91-02
Description of geophysical data in SKB database GEOTAB
Version 2
Stefan Sehlstedt
SGAB, Luleå
January 1991

TR 91-03
1. The application of PIE techniques to the study of the corrosion of spent oxide fuel in deep-rock ground waters
2. Spent fuel degradation
R S Forsyth
Studsvik Nuclear
January 1991

TR 91-04
Plutonium solubilities
I Puigdomènech[1], J Bruno[2]
[1]Enviromental Services, Studsvik Nuclear, Nyköping, Sweden
[2]MBT Tecnologia Ambiental, CENT, Cerdanyola, Spain
February 1991

TR 91-05
Description of tracer data in the SKB database GEOTAB
SGAB, Luleå
April, 1991

TR 91-06
Description of background data in the SKB database GEOTAB
Version 2
Ebbe Eriksson, Stefan Sehlstedt
SGAB, Luleå
March 1991

TR 91-07
Description of hydrogeological data in the SKB's database GEOTAB
Version 2
Margareta Gerlach (ed.)
Mark Radon Miljö MRM Konsult AB, Luleå
December 1991

TR 91-08
Overview of geologic and geohydrologic conditions at the Finnsjön site and its surroundings
Kaj Ahlbom[1], Sven Tirén[2]
[1]Conterra AB
[2]Sveriges Geologiska AB
January 1991

TR 91-09
Long term sampling and measuring program. Joint report for 1987, 1988 and 1989. Within the project: Fallout studies in the Gideå and Finnsjö areas after the Chernobyl accident in 1986
Thomas Ittner
SGAB, Uppsala
December 1990

TR 91-10
Sealing of rock joints by induced calcite precipitation. A case study from Bergeforsen hydro power plant
Eva Hakami[1], Anders Ekstav[2], Ulf Qvarfort[2]
[1]Vattenfall HydroPower AB
[2]Golder Geosystem AB
January 1991

TR 91-11
Impact from the disturbed zone on nuclide migration – a radioactive waste repository study
Akke Bengtsson[1], Bertil Grundfelt[1],
Anders Markström[1], Anders Rasmuson[2]
[1]KEMAKTA Konsult AB
[2]Chalmers Institute of Technology
January 1991

TR 91-12
Numerical groundwater flow calculations at the Finnsjön site
Björn Lindbom, Anders Boghammar,
Hans Lindberg, Jan Bjelkås
KEMAKTA Consultants Co, Stockholm
February 1991

TR 91-13
Discrete fracture modelling of the Finnsjön rock mass
Phase 1 feasibility study
J E Geier, C-L Axelsson
Golder Geosystem AB, Uppsala
March 1991

TR 91-14
Channel widths
Kai Palmqvist, Marianne Lindström
BERGAB-Berggeologiska Undersökningar AB
February 1991

TR 91-15
Uraninite alteration in an oxidizing environment and its relevance to the disposal of spent nuclear fuel
Robert Finch, Rodney Ewing
Department of Geology, University of New Mexico
December 1990

TR 91-16
**Porosity, sorption and diffusivity data
compiled for the SKB 91 study**
Fredrik Brandberg, Kristina Skagius
Kemakta Consultants Co, Stockholm
April 1991

TR 91-17
**Seismically deformed sediments in the
Lansjärv area, Northern Sweden**
Robert Lagerbäck
May 1991

TR 91-18
**Numerical inversion of Laplace
transforms using integration and
convergence acceleration**
Sven-Åke Gustafson
Rogaland University, Stavanger, Norway
May 1991

TR 91-19
**NEAR21 - A near field radionuclide
migration code for use with the
PROPER package**
Sven Norman[1], Nils Kjellbert[2]
[1]Starprog AB
[2]SKB AB
April 1991

TR 91-20
**Äspö Hard Rock Laboratory.
Overview of the investigations
1986-1990**
R Stanfors, M Erlström, I Markström
June 1991

TR 91-21
**Äspö Hard Rock Laboratory.
Field investigation methodology
and instruments used in the
pre-investigation phase, 1986-1990**
K-E Almén, O Zellman
June 1991

TR 91-22
**Äspö Hard Rock Laboratory.
Evaluation and conceptual modelling
based on the pre-investigations
1986-1990**
P Wikberg, G Gustafson, I Rhén, R Stanfors
June 1991

TR 91-23
**Äspö Hard Rock Laboratory.
Predictions prior to excavation and the
process of their validation**
Gunnar Gustafson, Magnus Liedholm, Ingvar Rhén,
Roy Stanfors, Peter Wikberg
June 1991

TR 91-24
**Hydrogeological conditions in the
Finnsjön area.
Compilation of data and conceptual
model**
Jan-Erik Andersson, Rune Nordqvist, Göran Nyberg,
John Smellie, Sven Tirén
February 1991

TR 91-25
**The role of the disturbed rock zone in
radioactive waste repository safety and
performance assessment.
A topical discussion and international
overview.**
Anders Winberg
June 1991

TR 91-26
**Testing of parameter averaging tech-
niques for far-field migration calculations
using FARF31 with varying velocity.**
Akke Bengtsson[1], Anders Boghammar[1],
Bertil Grundfelt[1], Anders Rasmuson[2]
[1]KEMAKTA Consultants Co
[2]Chalmers Institute of Technology

TR 91-27
**Verification of HYDRASTAR. A code for
stochastic continuum simulation of
groundwater flow**
Sven Norman
Starprog AB
July 1991

TR 91-28
**Radionuclide content in surface and
groundwater transformed into breakthrough
curves. A Chernobyl fallout study in an
forested area in Northern Sweden**
Thomas Ittner, Erik Gustafsson, Rune Nordqvist
SGAB, Uppsala
June 1991

TR 91-29
**Soil map, area and volume calculations in
Orrmyrberget catchment basin at Gideå,
Northern Sweden**
Thomas Ittner, P-T Tammela, Erik Gustafsson
SGAB, Uppsala
June 1991

TR 91-30
A resistance network model for radionuclide transport into the near field surrounding a repository for nuclear waste (SKB, Near Field Model 91)
Lennart Nilsson, Luis Moreno, Ivars Neretnieks, Leonardo Romero
Department of Chemical Engineering, Royal Institute of Technology, Stockholm
June 1991

TR 91-31
Near field studies within the SKB 91 project
Hans Widén, Akke Bengtsson, Bertil Grundfelt
Kemakta Consultants AB, Stockholm
June 1991

TR 91-32
SKB/TVO Ice age scenario
Kaj Ahlbom[1], Timo Äikäs[2], Lars O. Ericsson[3]
[1]Conterra AB
[2]Teollisuuden Voima Oy (TVO)
[3]Svensk Kärnbränslehantering AB (SKB)
June 1991

TR 91-33
Transient nuclide release through the bentonite barrier - SKB 91
Akke Bengtsson, Hans Widén
Kemakta Konsult AB
May 1991

TR 91-34
SIMFUEL dissolution studies in granitic groundwater
I Casas[1], A Sandino[2], M S Caceci[1], J Bruno[1], K Ollila[3]
[1]MBT Tecnologia Ambiental, CENT, Cerdanyola, Spain
[2]KTH, Dpt. of Inorganic Chemistry, Stockholm, Sweden
[3]VTT, Tech. Res. Center of Finland, Espoo, Finland
September 1991

TR 91-35
Storage of nuclear waste in long boreholes
Håkan Sandstedt[1], Curt Wichmann[1], Roland Pusch[2], Lennart Börgesson[2], Bengt Lönnerberg[3]
[1]Tyréns
[2]Clay Technology AB
[3]ABB Atom
August 1991

TR 91-36
Tentative outline and siting of a repository for spent nuclear fuel at the Finnsjön site. SKB 91 reference concept
Lars Ageskog, Kjell Sjödin
VBB VIAK
September 1991

TR 91-37
Creep of OFHC and silver copper at simulated final repository canister-service conditions
Pertti Auerkari, Heikki Leinonen, Stefan Sandlin
VTT, Metals Laboratory, Finland
September 1991

TR 91-38
Production methods and costs of oxygen free copper canisters for nuclear waste disposal
Hannu Rajainmäki, Mikko Nieminen, Lenni Laakso
Outokumpu Poricopper Oy, Finland
June 1991

TR 91-39
The reducibility of sulphuric acid and sulphate in aqueous solution (translated from German)
Rolf Grauer
Paul Scherrer Institute, Switzerland
July 1990

TR 91-40
Interaction between geosphere and biosphere in lake sediments
Björn Sundblad, Ignasi Puigdomenech, Lena Mathiasson
December 1990

TR 91-41
Individual doses from radionuclides released to the Baltic coast
Ulla Bergström, Sture Nordlinder
Studsvik AB
May 1991

TR 91-42
Sensitivity analysis of the groundwater flow at the Finnsjön study site
Yung-Bing Bao, Roger Thunvik
Dept. Land and Water Resources, Royal Institute of Technology, Stockholm, Sweden
September 1991

TR 91-43
SKB - PNC
Development of tunnel radar antennas
Lars Falk
ABEM, Uppsala, Sweden
July 1991

TR 91-44
Fluid and solute transport in a network of channels
Luis Moreno, Ivars Neretnieks
Department of Chemical Engineering,
Royal Institute of Technology, Stockholm, Sweden
September 1991

TR 91-45
The implications of soil acidification on a future HLNW repository.
Part I: The effects of increased weathering, erosion and deforestation
Josefa Nebot, Jordi Bruno
MBT Tecnologìa Ambiental, Cerdanyola, Spain
July 1991

TR 91-46
Some mechanisms which may reduce radiolysis
Ivars Neretnieks, Mostapha Faghihi
Department of Chemical Engineering, Royal
Institute of Technology, Stockholm, Sweden
August 1991

TR 91-47
On the interaction of granite with Tc(IV) and Tc(VII) in aqueous solution
Trygve E Eriksen, Daquing Cui
Royal Institute of Technology, Department of
Nuclear Chemistry, Stockholm, Sweden
October 1991

TR 91-48
A compartment model for solute transport in the near field of a respository for radioactive waste (Calculations for Pu-239)
Leonardo Romero, Luis Moreno , Ivars Neretnieks
Department of Chemical Engineering, Royal
Institute of Technology, Stockholm, Sweden
October 1991

TR 91-49
Description of transport pathways in a KBS-3 type repository
Roland Pusch[1], Ivars Neretnieks[2], Patrik Sellin[3]
[1] Clay Technology AB. Lund
[2] The Royal institue of Techonology Department of Chemical Engineering, Stockholm
[3] Swedisch Nueclear Fuel and Waste Management Co (SKB), Stockholm
December 1991

TR 91-50
Concentrations of particulate matter and humic substances in deep groundwaters and estimated effects on the adsorption and transport of radionuclides
Bert Allard[1], Fred Karlsson[2], Ivars Neretnieks[3]
[1]Department of Water and Environmental Studies, University of Linköping, Sweden
[2]Swedish Nuclear Fuel and Waste Management Company, SKB, Stockholm, Sweden
[3]Department of Chemical Engineering, Royal Institute of Technology, Stockholm, Sweden
November 1991

TR 91-51
Gideå study site. Scope of activities and main results
Kaj Ahlbom[1], Jan-Erik Andersson[2], Rune Nordqvist[2], Christer Ljunggren[2], Sven Tirén[2], Clifford Voss[3]
[1]Conterra AB
[2]Geosigma AB
[3]U.S. Geological Survey
October 1991

TR 91-52
Fjällveden study site. Scope of activities and main results
Kaj Ahlbom[1], Jan-Erik Andersson[2], Rune Nordqvist[2], Christer Ljunggren[2], Sven Tirén[2], Clifford Voss[3]
[1]Conterra AB
[2]Geosigma AB
[3]U.S. Geological Survey
October 1991

TR 91-53
Impact of a repository on permafrost development during glaciation advance
Per Vallander, Jan Eurenius
VBB VIAK AB
December 1991

TR 91-54

Hydraulic evaluation of the groundwater conditions at Finnsjön. The effects on dilution in a domestic well

C-L Axelsson[1], J Byström[1], Å Eriksson[1],
J Holmén[1], H M Haitjema[2]
[1]Golder Geosystem AB, Uppsala, Sweden
[2]School of Public and Environmental Affairs,
Indiana University, Bloomington, Indiana, USA
September 1991

TR 91-55

Redox capacity of crystalline rocks. Laboratory studies under 100 bar oxygen gas pressure

Veijo Pirhonen, Petteri Pitkänen
Technical Research Center of Finland
December 1991

TR 91-56

Microbes in crystalline bedrock. Assimilation of CO_2 and introduced organic compounds by bacterial populations in groundwater from deep crystalline bedrock at Laxemar and Stripa

Karsten Pedersen, Susanne Ekendahl,
Johanna Arlinger
Department of General and Marine Microbiology,
University of Göteborg, Göteborg, Sweden
December 1991

TR 91-57

The groundwater circulation in the Finnsjö area - the impact of density gradients

Part A: Saline groundwater at the Finnsjö site and its surroundings
Kaj Ahlbom
CONTERRA AB

Part B: A numerical study of the combined effects of salinity gradients, temperature gradients and fracture zones
Urban Svensson
CFE AB

Part C: A three-dimensional numerical model of groundwater flow and salinity distribution in the Finnsjö area
Urban Svensson
CFE AB
November 1991

TR 91-58

Exploratory calculations concerning the influence of glaciation and permafrost on the groundwater flow system, and an initial study of permafrost influence at the Finnsjön site - an SKB 91 study

Björn Lindbom, Anders Boghammar
Kemakta Konsult AB, Stockholm
December 1991

TR 91-59

Proceedings from the Technical Workshop on Near-Field Performance Assessment for High-Level Waste held in Madrid October 15-17, 1990

Patrik Sellin[1], Mick Apted[2], José Gago[3] (editors)
[1]SKB, Stockholm, Sweden
[2]Intera, Denver, USA
[3]ENRESA, Madrid, Spain
December 1991

TR 91-60

Spent fuel corrosion and dissolution

R S Forsyth[1], L O Werme[2]
[1]Studsvik AB, Nyköping, Sweden
[2]Swedish Nuclear Fuel and Waste Management
Co, Stockholm, Sweden
December 1991

TR 91-61

Heat propagation from a radioactive waste repository. SKB 91 reference canister

Roger Thunvik, Carol Braester
Royal Institute of Technology, Stockholm, Sweden
March 1991